DC LINK SENORLESS POWER CONTROL STRATEGY IN MICROGRID

A PROJECT REPORT

Submitted by

NEETHU PRASAD

TKM19EEPS07

to

the **APJ Abdul Kalam Technological University**

in partial fulfillment of the requirements for the award of the Degree

of

MASTER OF TECHNOLOGY

in

POWER SYSTEMS

DEPARTMENT OF ELECTRICAL AND ELECTRONICS ENGINEERING

T.K.M COLLEGE OF ENGINEERING

Kollam-5

2022

DEPARTMENT OF ELECTRICAL & ELECTRONICS ENGINEERING

THANGAL KUNJU MUSALIAR COLLEGE OF ENGINEERING
KOLLAM

CERTIFICATE

This is to certify that the Project report entitled **'DC LINK SENSORLESS POWER CONTROL STRATEGY IN MICROGID'** submitted by **'NEETHU PRASAD'** to the APJ Abdul Kalam Technological University in partial fulfillment of the requirements for the award of the Degree of Master of Technology in Power Systems, Electrical & Electronics Engineering is a Bonafede record of the project work carried out by her under our guidance and supervision. This report in any form has not been submitted to any other University or Institute for any purpose.

Prof. Jibi P Mathew
Assistant Professor [Internal Supervisor]
Dept. of Electrical and Electronics

E XTERNAL EXAMINER

Prof. SHANAVAS T.N
Associate Professor [PG Coordinator]
Dept. of Electrical and Electronics Engineering

Dr. Sabeena Beevi K
Associate Professor [HOD]
Dept. of Electrical and Electronics Engineering

ACKNOWLEDGEMENT

First of all, I am indebted to **GOD ALMIGHTY** for giving me bountiful blessings and strength throughout the period to complete this work successfully.

It is my privilege and pleasure to express my gratitude and indebtedness to **Dr. T Shahul Hameed,** Principal of TKM College of Engineering, and **Dr. Sabeena Beevi K,** Head of the Department, Dept. of EEE, for providing all the required resources for the completion of my project work.

I am greatly obliged to **Prof. Shanavas T. N,** Associate Professor, PG coordinator, Department of Electrical and Electronics Engineering, for his encouragement and support.

My heartfelt gratitude to **Prof. Jibi P Mathew**, Project guide, Assistant Professor, Department of Electrical and Electronics Engineering, for his valuable suggestions and guidance in designing and implementing this project.

I will be failing in duty if I do not acknowledge the authors of the references and other pieces of literature referred to in this project.

I show my extreme gratitude to all faculty member and technical staff in Electrical and Electronics Dept for providing all the help and necessary facilities to complete the project work and my deep hearted cheers to my parents and all my friends who extended their support and co-operation towards the successful completion of the project.

NEETHU PRASAD

ABSTRACT

The dependency of the energy market on renewable energy sources has grown rapidly over the past few years, especially photovoltaic systems. Also, microgrid is an area of interest as it can be used as an effective complementary of power grid. But microgrids face protection, reliability, and stability issues, so control should be prudent. Voltage-oriented control (VOC) and direct power control are the common methods for active and reactive power management of grid-connected PV systems. The main aim of this project is to develop a DC link sensor less control strategy for the microgrid. The first DC-DC converter stage of the system incorporates adaptive 'perturb and observe' maximum power point tracking. In the second stage, the DC link sensor less control is used to control the inverter. The proposed system uses a system loss model to generate the control signal. In this project, for a typical microgrid-connected PV system, the proposed model is designed and simulated in MATLAB SIMULINK. And the performance of the system is analysed and compared with the conventional VOC system. As an outcome, eliminating the DC-link high voltage sensor enhances the transient response and system stability under loading and reduces system size and cost.

CONTENTS

CHAPTER 1
INTRODUCTION

1.1 GENERAL BACKGROUND

The Better use of renewable energy sources and highly decentralized load supply are made possible by microgrids. The integration of distributed generation from renewable sources into the electrical network, along the upgrading of electric loads, has had a significant impact on how the power system operates. Since the design of the control strategies can become extremely complex and is a significant research topic in this field, the development of control techniques for the operation and management of a microgrid presents a major challenge. A microgrid needs to manage its variables in order to operate safely, to ensure transient stability, to control the flow of power, and to pay attention to local load requirements within the network for example, control of frequency and voltage, enhancement of distributed generation, dependable operation, and robustness to network interruptions.

Due to the increasing cost, diminishing reserves, and environmental issues associated with fossil fuels, renewable energy sources now account for a good proportion of the world's energy production. Among the former, photovoltaic (PV) energy has attracted a lot of attention as a resource that can be expanded and used in rural regions and generates less noise and pollution. For the optimal use of the electric power, common distributed energy resources (DERs) are increasingly being connected to utilities. For connecting PV systems to the grid, a number of grid interfaces have been proposed, the most popular of which being the string inverter topology. It fixes the problems with the outdated centralized inverter system, which connects several PV strings to a single inverter and suffers from non-flexibility and power losses from MPPT mismatch. As an alternative, the string inverter approach connects several PV modules in a series configuration known as a string; each string has its own inverter, and the system may be expanded

by adding additional strings and the corresponding inverters. It is required to implement a comprehensive control strategy involving various time-scale It adhering to a hierarch control structure, in order to ensure the proper operation of a microgrid. Microgrids ensure effective and efficient integration of renewable energy. sources and proper management of storage components, both of which enhance the electrical systems' ability to produce quality power. Power electronic converters are being used more extensively to connect energy sources to the grid. They enable tightly regulated power flows and flexible operation methods, which are still the subject of much research, and they often raise other potential grid problems. Conventional control of active and reactive power in microgrid connected distributed resources include voltage-oriented control and direct power control.

Therefore, in order to perform power control using conventional control technique, PV voltage and current data are necessary. Additionally, measuring grid voltage and current as well as sensing DC-bus voltage for the outer DC-link voltage control loop are both required. However, in sensorless power control techniques, either grid voltage sensors can be eliminated or dc link voltage sensors. Various approaches for current control have been developed in recent years. Hysteresis current control is a grid voltage observer - based technique that is conceptually simple and doesn't require complex hardware or processing power. The interaction between the phases prevents the output current from being strictly confined within the hysteresis band, which makes it impossible to maintain high-quality output current. There have also been developed other methods that merely control the inverter utilizing grid current. These grid-connected inverters can operate without the need for a grid voltage sensor, but they are unable to maintain a high output current with just the grid current control.

1.2 MOTIVATIONS

Understanding the dc-link voltage is essential for power control strategies (vdc). The output current cannot follow its reference if the vdc information is incorrect. Consequently, vdc is a significant factor required to generate an output current of high quality. The dc link power control schemes are more complicated when a sensor is included, which causes a slow response time and higher

costs. To create a simplex, fast response system, it is crucial to investigate the sensorless dc link active and reactive power control approach

1.3THESIS MAIN OBJECTIVES

To develop a sensorless power control technique

To simplify the control structure and increase the reliability of the system.

To eliminate the DC-link voltage sensor, which will lower the overall system's cost

To provide a fast response with conventional Voltage oriented control.

1.4 ORGANIZATION OF THE THESIS

The entire thesis is organized as follows. It consists of seven chapters. Chapter 1 is a brief introduction of the thesis and the motivation and objectives about the same. Chapter 2 deals with the literature review about the several power control methods and the technical gaps associated with each of them. Chapter 3 gives an outline about the concept of several active power control methods. The basic information regarding the control technics indices and compares which all categories the control structure falls to, is discussed in it. Chapter 4 is the methodology followed in the thesis. The methodologies of control structure with two loops to control the inverter is discussed. Chapter 5discuss the proposed model with its maximum power point tracking method and sensorless control method considering the system losses. Chapter 6 shows the simulation diagram of the proposed model with design of various equipment associated with the system. Chapter 7.the results that are obtained from the simulated system is taken and compare the conventional control structure model with the proposed one. Finally, chapter 8 gives the conclusion and the future research scopes in this area

CHAPTER 2
LITERATURE SURVEY

The active and reactive power control of inverters connected to microgrids is a topic of extensive investigation. The most popular approaches, however, are voltage-age oriented control (VOC) and direct power control (DPC) [1]. The DPC technique is developed in accordance with the inaccuracy between the instantaneous values of active and reactive power and their references with knowledge of the position (angle) of the grid voltage. As a result, without the usage of a modulator, a look-up table can be utilized to determine the switching actions of the inverter. From the output, it is seen that the switching frequency of the DPC is variable, and the power waveform has a high level of ripple.

In [2] the researchers have done this pragmatic model for various applications. Numerous researchers have used the sensorless approach in addition to the standard method at the direct current side of the inverter (DC-link location) for many different applications. used this approach for the grid-connected inverter with fixed DC voltage source, as mentioned in. The grid voltage and output current were utilized by the writers of this literature to estimate the DC-link voltage, which approached relevant to the actual value. This control approach for a doubly fed induction generator in a wind energy conversion system was introduced by Naidu and Singh.

The VOC regulates the inverter control using two cascaded loops. The DC-link capacitor voltage is connected to the outer loop or voltage loop, and a proportional integral controller is used to generate the reference current for the inner loop or current loop. The currents are then regulated by two PI controllers, accounting for the active/reactive power control [3]. Due of their strong transient reaction, predictive control approaches have recently attracted greater attention. To enforce specific tasks, additional criteria and constraints might be introduced to the algorithm. This control technique, however, suffers from a computational complexity overhead and variable switching frequency

In [4] to reduce the amount of power lost when the power flow is altered (less than and more than) in their article, have demonstrated a single VSC at synchronous speed. For boost-type rectifiers, they have offered a sensorless power factor correction control method. By doing so, this endeavor enhances the system's transient response by getting rid of the voltage loop proportional integral (pi) controller. A sensorless strategy for GCPVS was given by Zak- Zouk et, limiting the system to a single phase. The shortcomings of this approach include the presence of the line frequency of the second order and the failure to transmit the bulk power. transformer conditions.

A number of measures must be met for PV string interface with the grid to be successful. The performance of a PV source depends on the operating irradiance and temperature conditions, therefore maximum power point tracking (MPPT) of the PV string is crucial to optimize system efficiency. Additionally, grid current control and voltage regulation at the inverter DC-link are crucial. As a result, there are two topologies: single-stage and two- stage topologies as cited in [8]. A single inverter stage performs PV MPPT and PV-grid interface duties in the single-stage system. Voltage ripples on the DC bus caused by double line-frequency grid power fluctuations owing to single-phase connection are a significant downside of this design.

According to [9], the grid connected PV systems can be vector controlled to individually regulate both active and reactive powers. The rotor position sensor was employed as most failures occur in the rotor position angle. This rotor position sensor has always been the target of numerous attempts. The computation of the rotor flux using rotor voltage and current is the main challenge of the suggested approach. They propose a straightforward position sensorless solution that performs admirably at synchronous speed.

In [10], an open-loop method for predicting the rotor position uses the straightforward mathematical equations of the observed voltages and currents. This might not perform well in all circumstances. To reduce the inaccuracy between the reference model and the adaptive model, the suggested solution in [9] uses a closed-loop system based on the MRAS (model reference adaptive system) algorithm. This paper employs a sensorless MRAS algorithm based on stator flux. However, the BESS (battery energy storage system) has undergone a full revolution in terms of its applicability in high-power ratings.

each element. This will benefit the end-users and power system operators to reduce the component failures and hence the cost associated with the removal of the failure.

In [11] the method is based on sensorless MPPT control scheme fact that PV generated power and grid side power should be in balance as the DC-link voltage is kept constant by the controller action at steady-state. As a result, the amplitude of the grid current will be forced to match the power generated by the PV. Therefore, PV MPPT can be achieved without PV sensors by adjusting the chopper duty cycle to optimize the line current amplitude. However, compared to the traditional technique, which directly senses PV power, the total system response degrades.

CHAPTER 3
POWER CONTROL MODELS

3.1 INTRODUCTION

This chapter focuses on the basic introduction of various power control methods for microgrid connected photovoltaic system, which can be implemented with information from grid side without grid voltage sensor or converter side sensors. Some power control techniques can be either with senor or sensorless for obtaining current information for power control.

3.2 SENSORLESS POWER CONTROL OPERATION

Normally, the pulse width modulation two stage rectifier needs three kinds of sensors:

1. **DC-voltage sensor**
2. **AC-line current sensors**
3. **AC-line voltage sensors**

The sensorless techniques benefit the system from a technical and financial standpoint by simplifying it and isolating the power circuit from the control system, as well as by ensuring dependability and cost efficiency. However, the rectifier application differs from the inverter operation for the following reasons: Zero vector will short the line power; The line operates at constant frequency 50Hz and synchronization is necessary. The possibility of reducing the number of the expensive sensors has been studied, particularly in the field of motor drive application.AC voltage and current sensorless, AC current sensorless, and AC Voltage sensorless are the most popular methods for decreasing the number of sensors

3.2.1 GRID VOLTAGE SENSORLESS CONTROL

It is commonly known that current sensors can be reduced, particularly for AC drives. Using the reference voltage vector and DC link current information for each PWM cycle, the two-phase currents can be computed. The biggest operational issue with the system is the lack of comprehensive protection. The zero vectors (U0, U7) present no current in the DC-link, specifically for PWM rectifier, and simultaneously short circuit three-line phases. The newly enhanced method is to sample the DC-link current a few times throughout a switching period, as shown in. Figure illustrates the fundamentals of current reconstruction as well as the voltage vector patterns that determine the flow of current.

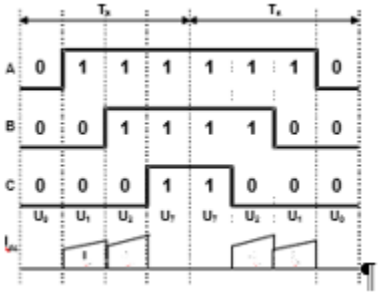

Fig. 3.1 Pulse width modulation signals and DC link current in sector 1

Table 3.1 Relationship between voltage vectors dc-dc converter, DC line current.

Voltage sensor	DC link current i_{dc}
U1(100)	+Ia
U2(110)	-Ic
U3(010)	+Ia
U4(011)	-Ia
U5(001)	+Ic
U6(101)	-Ib
U0(000)	0
U7(111)	0

Using the smallest pulse width possible for DC-link current collection is the main problem with AC current estimation. When one of the two active vectors is missing or just briefly employed, it manifests. Phase current cannot be reconstructed in such a situation. This arises when one of the six possible active vectors in reference voltage vectors passes, or when the modulation index is low. The shortest possible time to obtain an accurate estimate relies on the system's speed, delays, cable length, and dead time. Adjusting the PWM-pulses or allowing for a period of time in which no current information is present are two possible solutions to the issue. As a result, better compensation helps determine the mistake caused by the PWM pulse modification and then correcting it during the subsequent switching period.

Despite being less expensive, the AC voltage and current sensorless methods have a number of drawbacks, including higher current ripple contents, issues with discontinuous modulation and overmodulation mode, sampling being presented only a few times per switching state, which is technically inconvenient, and not reporting unbalance and startup conditions.

3.2.2 SENORLESS ESTIMATION OF GRID VOLTAGE AND VIRTUAL FLUX

Recently, the grid side sensorless technology has gained increasing popularity. This is due to the possibility of reduced control system costs, increased modularity, and in some specific circumstances, increased GCI system reliability. In order to preserve the regular grid-connection operation for wind power applications, an efficient backup voltage- sensorless control system is needed. This is considering that the GCI's voltage sensors are malfunctioning. The average of the grid voltage, which can be seen as a virtual flux, is the most widely used and practical approach for such grid side voltage -sensorless operation (VF).

A voltage estimator must be able to accurately predict voltage in imbalanced conditions and with existing voltage distortion with harmonics. Not only the fundamental component but also Conventional also, the voltage imbalance and harmonic components should be accurately estimated. A higher overall power factor is produced. It is possible to determine the voltage across the inductance by varying the current. By referencing the rectifier input voltage and the computed voltage drop across the inductor, one can then estimate the line voltage.The problem of this

strategy is that it differentiates the current, which introduces noise into the current signal. To prevent this, a voltage approximation based on the power estimation can be implemented

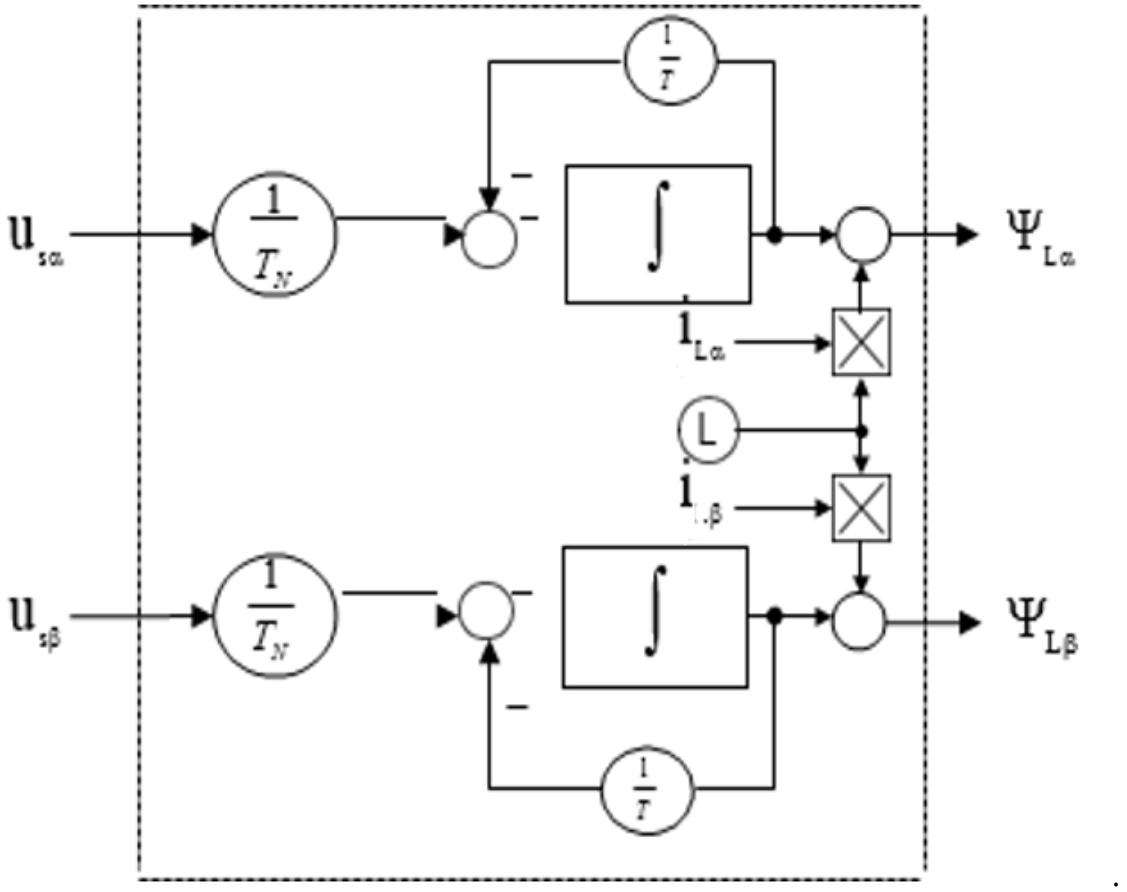

Fig. 3.2 First-order filter-equipped virtual flux estimator

Different observers that exclusively take into account the information of the converter side current and the dc link voltage have been investigated for the VF estimate. Realizing the pure integration is the main problem with VF estimate. Numerous developed approaches for the implementation of practical integration have been offered, as the direct approaches of pure integration realization are vulnerable to estimation drift and saturation. Common low-pass or band-pass filters made to

imitate assimilation for the utility grid at fundamental frequency and the low voltage side of the dc bus are incremented by the methods are the foundation of conventional estimating techniques. In every switching state the power is estimated many times while the current is sampled. In traditional space vector modulation (SVM) for three-phase voltage source converters, the AC currents are sampled during the zero-vector stages because there is no transition noise present and a filter in the current loop for the current control loops can be omitted. However, these techniques are incredibly susceptible to changes in grid frequency.

3.2.3 DIRECT POWER CONTROL

Controlling a PWM rectifier can be seen as a twofold issue with grid-connected PV system vector control. Works on this type of PWM converter have been presented as number of different control schemes. Although both control systems can produce near-sinusoidal current waveforms and high-power factors, their underlying principles are different. Particularly popular and continually developed and enhanced is the Voltage-Oriented Control (VOC), this, through internal current control loops, guarantees great dynamics and static performance. As a result, the quality of the used current control method greatly influences the final configuration and performance of the VOC system. Direct Power Control (DPC), a differential control method, is based on immediate active

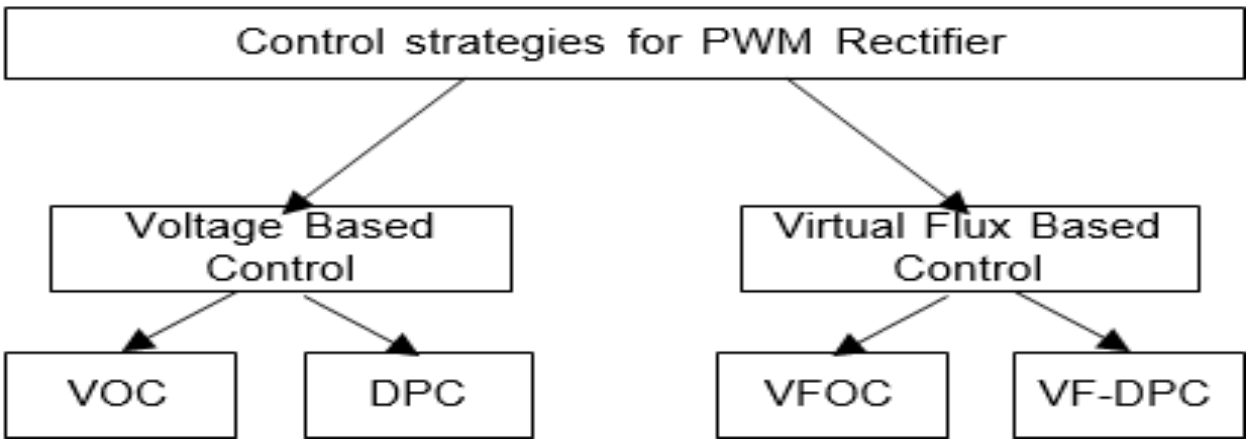

Fig. 3.3 Classification of control methods for pulse width rectifier

The primary concept underlying Direct Torque Control (DTC), which was first proposed for induction motors and later developed, is comparable to Direct Power Control (DPC). Instantaneous active (p) and reactive (q) currents are regulated instead of torque and stator flux.

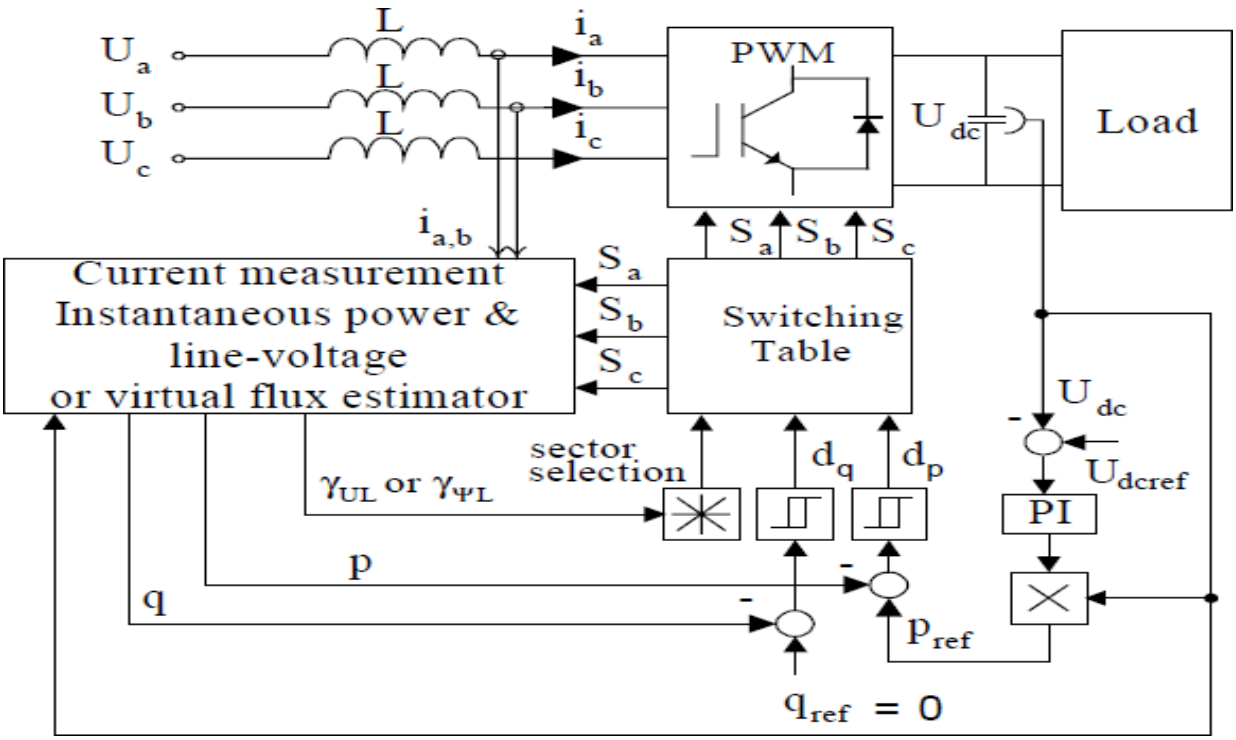

Fig. 3.4 Block scheme of Direct power control

3.2.4 DPC BASED ON SENSORLESS GRID VOLTAGE ESTIMATION

In Voltage-based power estimation for DPC the sum of three phase voltages and currents determines the instantaneous active and reactive powers. In an AC voltage sensorless system, the instantaneous active (p) and reactive power (q) values are approximated. In contrast to the reactive power q, which is determined as its vector product, the active power p is the product of the current and voltage. In both equations, the inductance's power is expressed by the first portion while the rectifier's power is represented by the second. Understanding line voltage is crucial since the AC-line voltage sector is required to read the switching table. As soon as the estimated active and

reactive power levels are estimated and the AC-line currents are known. This power estimating approach, despite its simplicity, has major drawbacks, including:

a) This power estimating approach, despite its simplicity, has major drawbacks, including:

b) The switching status affects how much power is estimated. Therefore, due to the high probability of prediction mistakes, power and voltage calculations should be avoided right before switching.

3.2.5 DPC BASED ON SENSORLESS VF GRID VOLTAGE ESTIMATION

The virtual flux technique is used to estimate the input of momentary active and reactive power as well as the three-phase utility voltage. The idea behind VF-DPC is to operate the two-phase ac-dc converter by combining the direct power control (DPC) scheme with the input alternating current source estimate approach. An effective approach for determining the virtual flux components and the selection of converter voltage vectors is necessary for the proper operation of the VF- DPC. A simple low-pass filter is added to the system to address the errors in phase and magnitude brought on by the virtual flux estimate technique. The VF-DPC is in charge of managing the line current harmonics, power factor, and dc-link output voltage by regulating the input of instantaneous active and reactive power. The construction of the VF-control DPC is shown in Figure 3.5. Equation's transformation matrix is used to convert any further defined three-phase electrical variables in abc-coordinates into stationary -αβ coordinates. Figure indicates that, in contrast to typical DPC, no line voltage sensor is needed. This controller has a number of benefits, one of which is that it leads to less Total Harmonic Distortion (THD) than the DPC technique. As a result, it is chosen such that the active and reactive powers may be controlled smoothly during each sector.The number of sensors can be decreased to reduce its size and cost. Because a quick microprocessor and analog to digital converter are required, this control approach of a component, has attempted some drawbacks. Microprocessors that run faster produce more heat and need active cooling techniques. In particular, insulted gate bipolar transistor (IGBT) devices can suffer significant damage if heat is not dissipated effectively from the CPU and other components. vigorous cooling methods are

needed due to increased heat generation. Without adequate heat dissipation, the CPU or other components may suffer serious harm, especially if the devices use insulted gate bipolar transistors (IGBTs).

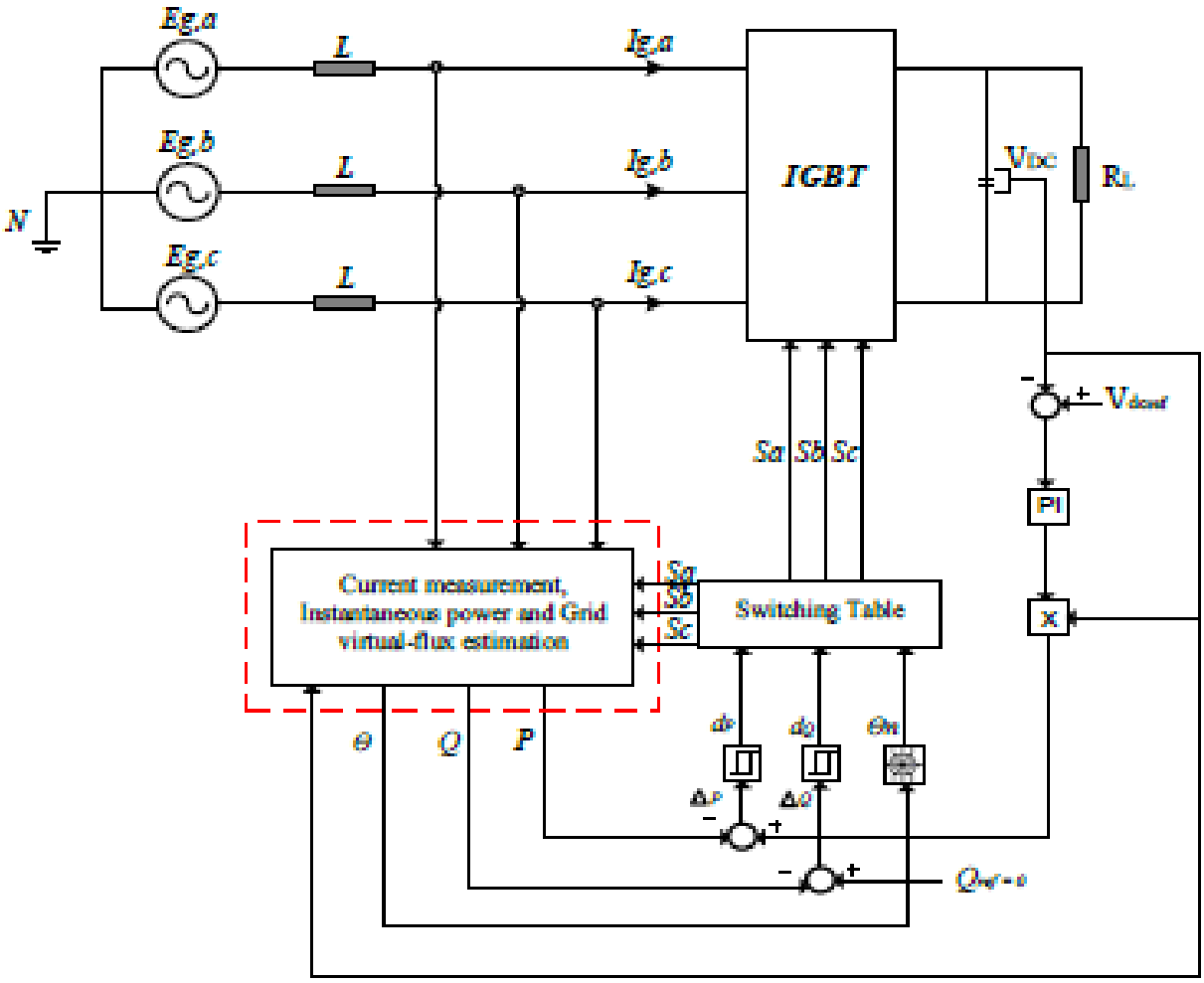

Fig. 3.5 Control structure of virtual flux direct power control

Two of the four potential active vectors are incorrect, for example, when the instantaneous reactive power vector is near a sector boundary. These flawed vectors can only change the active power that is being used right now; they cannot fix the reactive power problem. On a current, this is

immediately visible. A few techniques are well recognized for enhancing DPC behavior in sector bonders. One is to increase the number of sectors or hysteresis levels.

3.2.6 VIRTUAL FLUX ORIENTED POWER CONTROL

Based on coordinate translation between stationary - and synchronous rotating d-q reference systems, the Voltage Oriented Control (VOC) and Virtual Flux Oriented Control (VFOC) for controls systems PWM rectifier, same like in FOC of an induction motor. Both solutions rely on internal current control loops to guarantee good static performance and rapid transient reaction. As a result, the effectiveness of the present control method used heavily influences the eventual system setup and effectiveness. Hysteresis control's average switching frequency fluctuates with load current, creating an uneven and erratic switching pattern that puts additional strain on switching devices and presents challenges for the design of LC input filters. The d-q synchronous controller, one of the regulators that is now being utilized for high performance current control, regulates direct current quantities, removes steady state error.

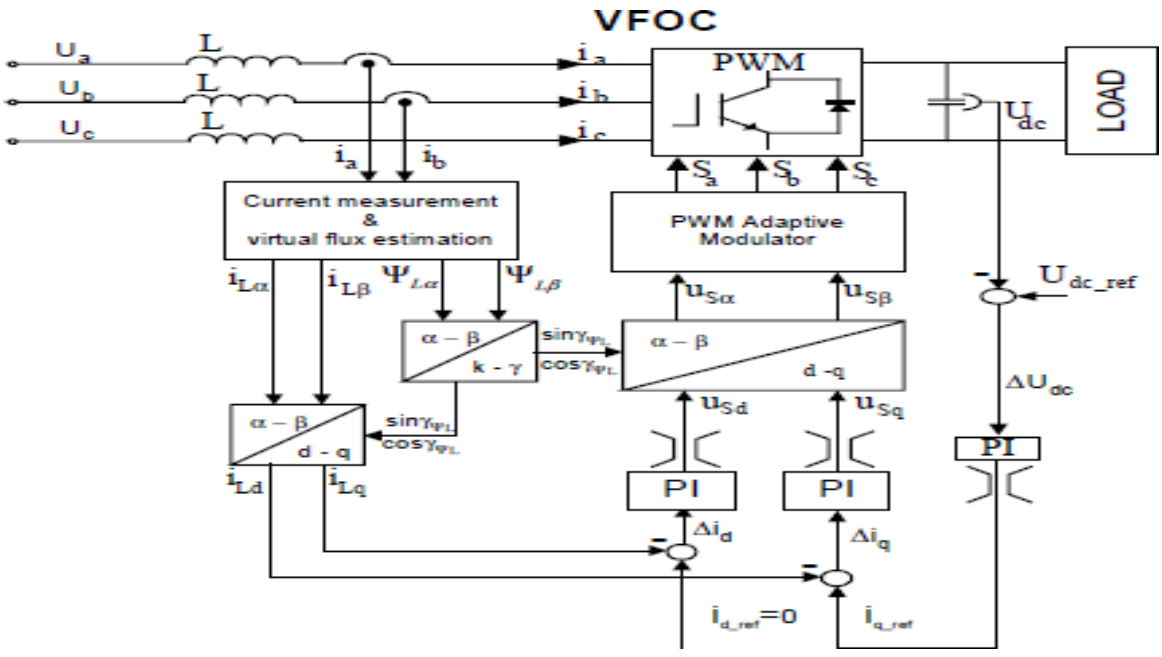

Fig. 3.6 AC voltage sensorless VOC

3.3 DC LINK VOLTAGE SENSORLESS CONTROL

Over the past two decades, electronic control and power electronics have been extensively used to regulate the net current and voltage of DG systems. As a result of the quicker sampling and computing speeds provided by microprocessors and digital signal processors (DSP), numerous novel sensorless solutions for inverters and rectifiers have been created. In order to obtain the current data from DC and AC voltage sensors, the current sensorless control approaches use a system model.

The current differential equations are used by the sensorless AC voltage approaches to obtain the voltage data. A sensorless control of the rectifier is suggested based on a dualism with the pulse width modulation (PWM) inverter-fed induction motor control. The PI current controller is modified to estimate the position of the line voltage in order to obtain the direction error signal controlling an observer.

Additionally, techniques without DC voltage sensors are being created. The DC voltage for single-phase systems is produced by an especially created differentiator circuit using the inductor current. The inductor current, AC voltage, and differential functions are utilized to calculate the DC voltage for three-phase systems. However, sampling noise and the filter circuit cause a discrepancy between the waveforms of the digital signal and the actual output of the inverter. This mismatch will result in inaccuracies in the differential computation, which will prevent the output current's total harmonic distortion (THD) from meeting the IEEE standard.

3.3.1 SPECIAL DESIGNED DIFFERENTIOR CIRCUIT

Simply detecting an input ac voltage waveform will allow you to construct a simple sensorless single-phase PFC converter. The control system can be built without using the direct current voltage or direct current sensors used in the standard PFC converter. The boost chopper circuit's command input signal directly controls the dc voltage. Due to a minimal dependence between the circuit parameters, the dc voltage regulation is minimal.

The sinusoidal current pattern and ac voltages may be in phase. The control system is very straightforward, the implementation of the system is also very concise, and it can be quickly put together because complex signal processing or computations, like derivative operation, are not necessary.

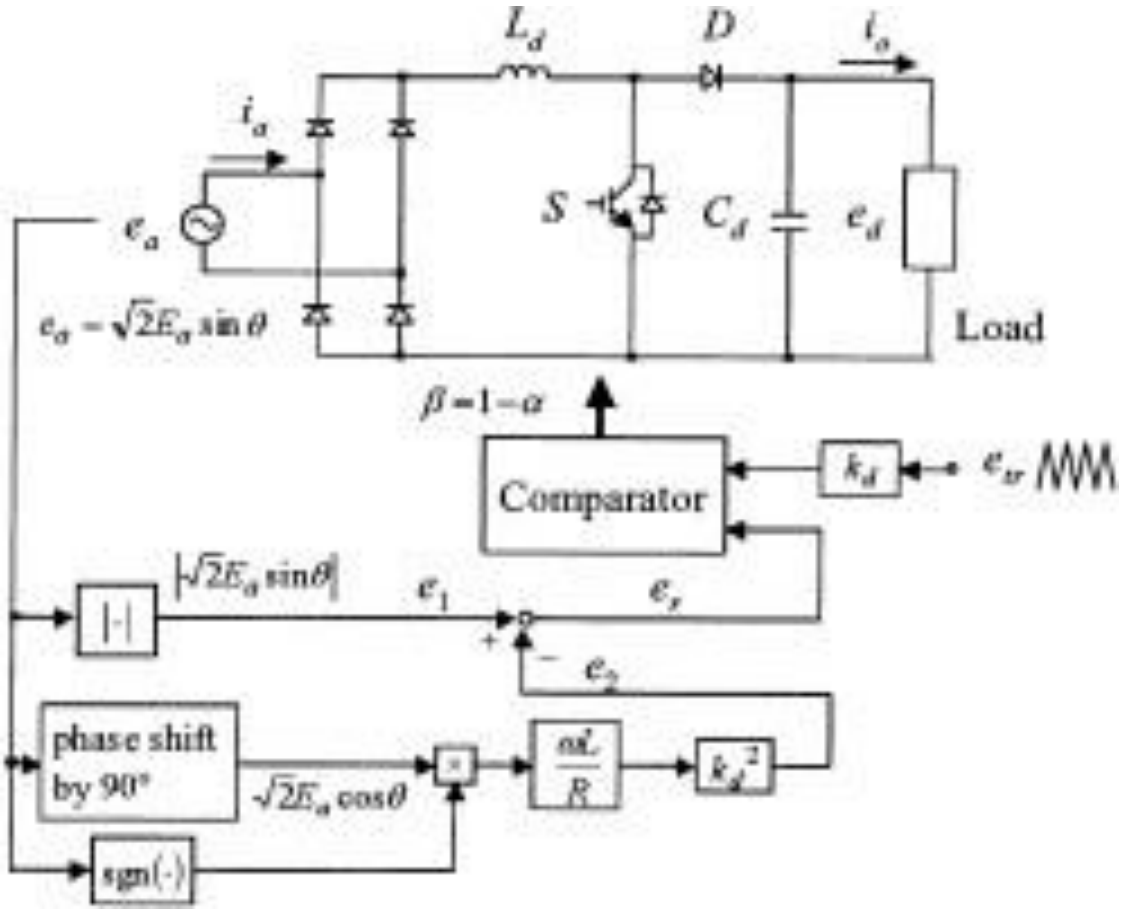

Fig. 3.7 PFC dc link converter sensorless control system

Only the ac line voltage is monitored and employed in this control system to provide the switching signal for the switching device. Therefore, in the control system, both the alternating current sensor and the dc voltage sensor can be eliminated. Power factor converter use the sensorless control.

3.2.2 COMPARASION OF MAINS AND RECTOR VOTAGE

A PWM rectifier controller without main voltage and direct current-side voltage measurement is proposed. This controller, which also offers the above benefits, is based on a modified version of the voltage sensorless technology for single-phase PWM rectifiers and a method that was put out to address the inherent issues with three-phase systems. The observed currents and their time-dependent derivatives are used to determine the main voltage and direct current-voltage values, both of which are essential for controlling instantaneous current.

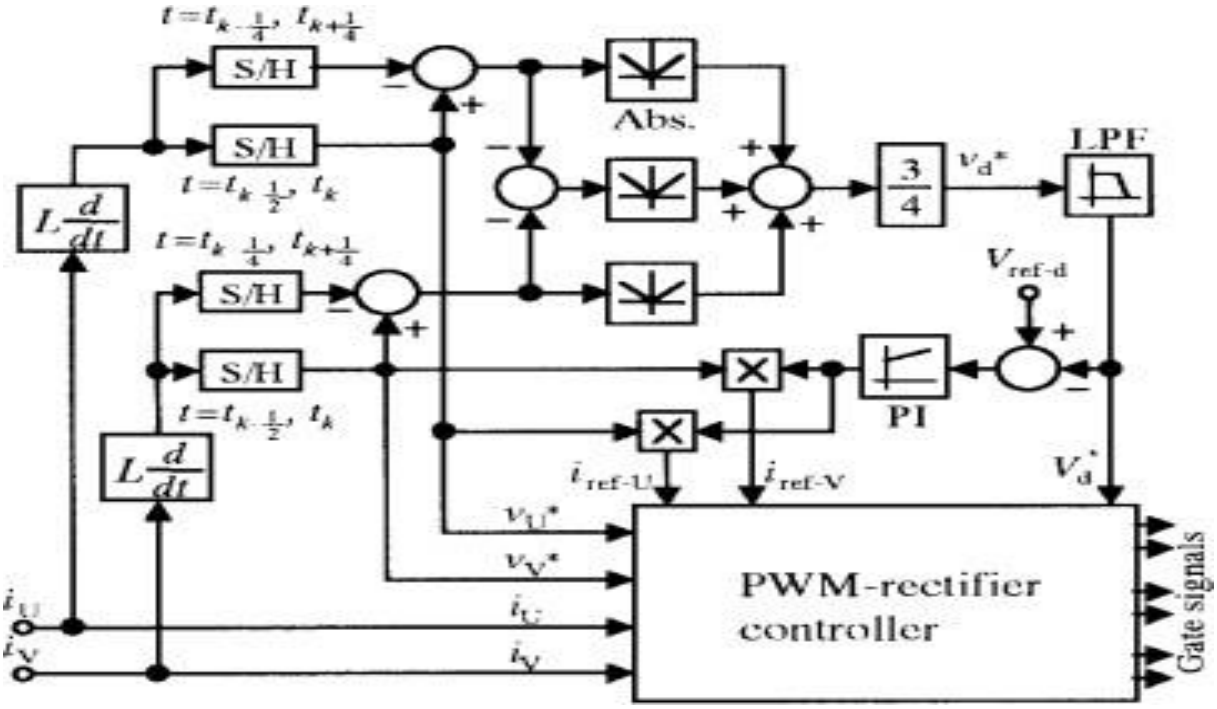

Fig. 3.8 Sensorless dc voltage estimation

The voltage level can be utilized to determine the mains voltage when the primary side of the bridge is shorted. By multiplying the reactors inductance and the derivative of the measured line current, or by using an additional winding on the input reactor, the reactor voltage can be computed with ease. By calculating the difference between the estimated voltage level and the reactor voltage

when the mains sides and dc side of the bridges are electrically linked, it is feasible to determine the dc-side voltage. Therefore, the if a splitter is employed in the controller to calculate the gradient of the line current, the rectifier can operate without any voltage sensors. The voltage level can be utilized to determine the mains voltage when the bridge's mains side is shorted. By compounding the reactors inductance and the derivation of the measured line current, or by using an additional winding on the input reactor, the reactor voltage can be computed with ease. By calculating the difference between the estimated voltage level and the reactor voltage when the mains end and dc side of the bridges are electrically linked, it is feasible to determine the dc-side voltage. Therefore, if a differentiator is employed in the controller to calculate the voltage, the rectifier runs without any voltage sensors.

3.3.3. IMPEMENTATION OF VIRTUAL SENSORS

Three separate sensors are used by PWM active inverters: one for voltage level and two for input currents. The converter's overall cost divided by the complexity, weight, and associated electronic

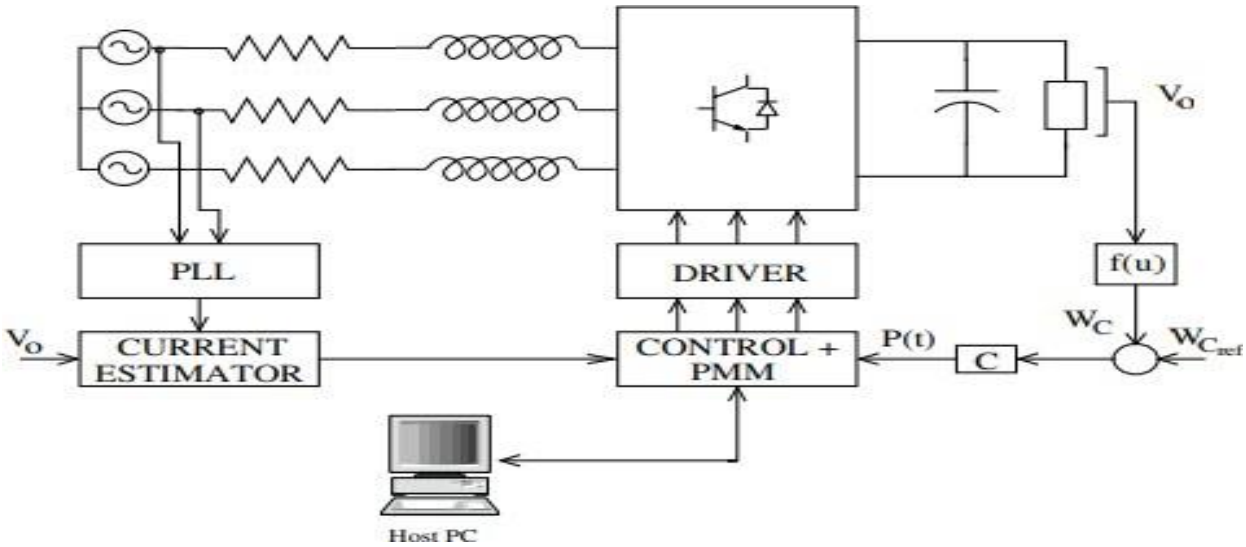

Fig. 3.9 Schematic diagram of the control of active converter

control circuits of the sensor systems grow as the cost of the electronic devices (microprocessors, IGBT) drops, which also causes a modest decline in the system's reliability. By using virtual

sensors, or computing input currents using the data provided by a single current sensor (often located inside the dc link) and the active rectifier state, for instance, good performance has been achieved. The method described here use an input-current model-based controller that calculates load conductance without the usage of current sensors for estimate and forecast of control and line current.

CHAPTER 4

SENSORED CONTROL APPROACH

4.1 INTRODUCTION

This chapter deals with detailed descriptions of conventional voltage oriented active and reactive power control in a photovoltaic microgrid connected systems. Modelling of DC DC converter along with MMPT, inverter control with voltage-oriented control, addition of load into the system to check for transient response of the system

4.2 TWO STAGE THREE PHASE GRID CONNECTED PV SYSTEM

The envisaged three-phase two-stage GCPVS's elaborate structure is shown in fig 4.1

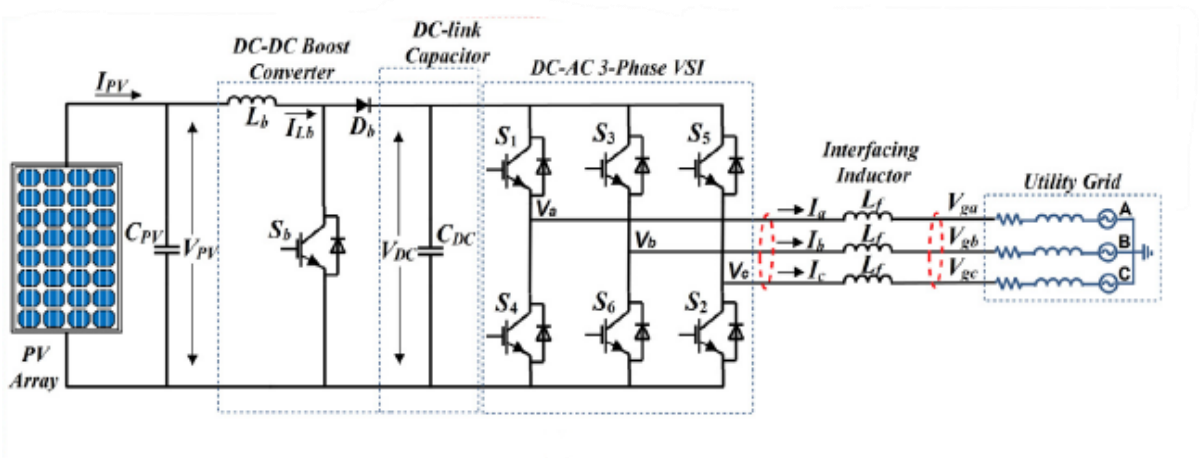

Fig. 4.1 A three-phase two-stage GCPVS

This system, which has a rated capacity of 1 to 30 kW, is commonly used for both residential and commercial purposes. This system consists of a grid, filters (three interface inductors), a voltage source inverter, a DC-link capacitor, PV array, and boost converter. Additionally, these parts are separated into two stages. VSI, which serves as a utility side converter, and a PV side boost converter make up the first stage. The solar photovoltaic array is used as an input of the dc-dc converter and is made up of a combination of modules arranged in series and parallel to produce the desired input current and voltage. As a converter in between a PV array and a VSI, the boost converter is used. It raises the PV array's voltage level to ensure that VSI obtains an adequate voltage for the GCP VS. The operational points, VMPP (voltage at maximum power point) and IMPP (current at maximum power point) at corresponding PMPP, are chosen using the MPPT method (power at maximum power point). The MPPT algorithm creates the PWM pulse for the boost converter switch based on operating voltage and current. A PWM implemented VSI is employed in the second step. Harmonic distortion is reduced to a minimum when PWM is used with VSI.

The voltage source converter in this system performs a number of tasks, namely

(a) converting DC to AC power

(b) independently controlling active and re-active current

(c) synchronizing with the grid

(d) Furthermore, voltage-oriented control is used to carry out these tasks.

4.3 PV ARRAY FORMULATION

A photovoltaic array is a current-generating device made up of photovoltaic modules that are comparable to one another and are stacked either in series, parallel, or both. According to Fig. 3, maximum power is calculated as the sum of all threads connected in parallel plus all modules connected in series. The boost converter is given the obtained Vmpp and Impp at a specific Pmpp

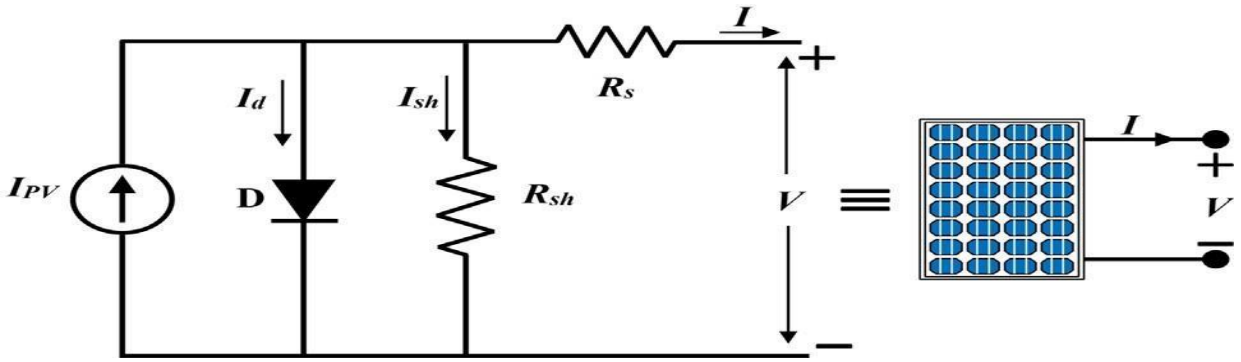

Fig.4.2 PV module with a single diode model

The PV array's maximum power is described as

$$P_{mpp} = (N_{ser} \times V_{mpp}) \times (N_{par} \times I_{mpp}) \quad (4.1)$$

where N_{ser} and N_{par} are used to construct a PV array in series and parallel.

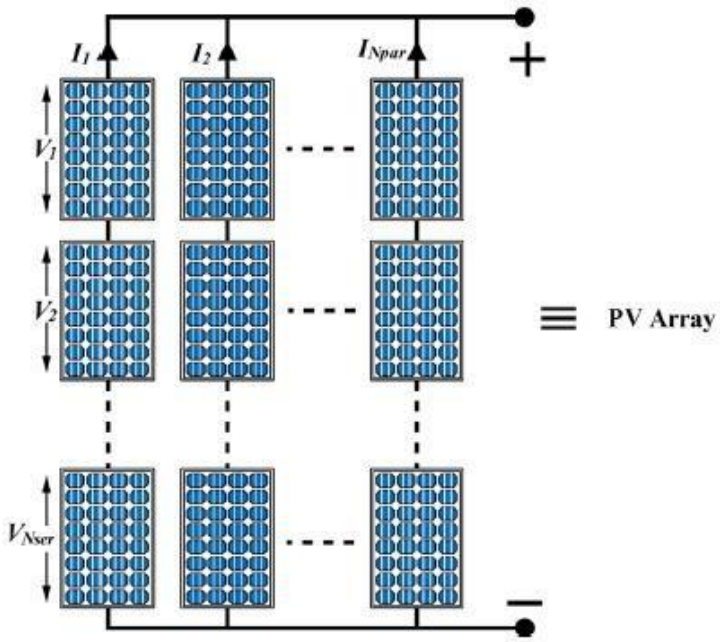

Fig. 4.3 Parallel and series connection of photovoltaic array

4.4 FORMULATION OF BOOST CONVERTER

The storage components and switches that are employed in the system have an impact on the parameter design and system performance. A controlled switch (Sb) and an uncontrolled switch (Db) with their respective functions for two switching instants are present in the boost converter portion. Sb is ON and Db is OFF for the first infinitesimal time interval, dTs.

$$VDC = \frac{1}{1- D} Vpv \quad (4.2)$$

This represents the proposed boost converter's small signal model for the GCPVS. Input voltage (Vpv) and duty cycle are the two input factors that influence how the subsystem (boost converter) operates. The target output value for this subsystem, represented by in steady position, is VDC, determines PV's constant value while d changes. The DC-AC VSI's input DC voltage is VDC. The selection of the appropriate component determines how well VSI for grid integration works (the full capacity of switches and interfacing inductors) and an effective operation-level control technique. The control strategy depends on the mathematical modelling of the structure in a chosen environment, and the component choice depends on the power transfer rating (either a stationary reference frame or a natural reference frame).

4.5 FORMULATION OF VOLTAGE SOURCE INVETER

The grid-connected voltage source inverter is mathematically represented as illustrated in Fig.4.4, where Va, Vb, and Vc are the inverter's terminal voltages, Vga, Vgb and Vgc are the grid voltages, and Lf is taken into account as the equivalent interface inductors for each of the three phases. To create a synchronously rotating reference frame, the preceding equation is further changed (SRF). Since the active and reactive power are no longer connected in this reference frame, the controller can be regulated independently. From the inverter's input side to its output side, the voltage regulation must be accomplished. Controlling the system's input of both active and reactive power

will help to achieve this integrated VSI, boost converter, and PV array mathematical models serve as a basis for the power control of the GCPVS in SRF

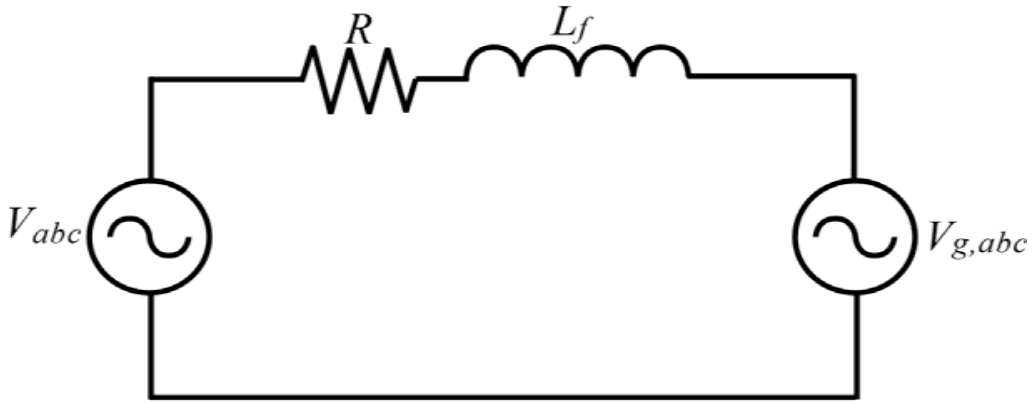

Fig. 4.4 Equivalent circuit of a three phase

Therefore, the discussion in the following section will focus on how the MPPT control, dc-dc converter control, and grid-integration regulate of voltage source inverter are further implemented from the chosen control factors, such as input voltage and current from the PV system, duty cycle for the boost converter, and control framework for the grid-integrated voltage source inverter.

4.6 CONTROL STRATEGY FOR GRID CONNECTED PV SYSTEM

Boost converter and the inverter topologies needs the control structure. Maximum power point tracking is implemented in dc-dc converter for better tracking of the power and to increase the efficiency of the system. Another control structure is to be implemented at inverter to control the active and reactive current. Thereby the active and reactive power.

4.6.1 CONTROL OF DC-DC CONVETER WITH MPPT

Solar PV panels are coupled to a DC-to-DC boost converter, enhances the input voltage to the necessary level while having its pulse controlled by MPPT. The system uses MPPT to track the maximum power. To extract the maximum solar PV power generation, the system employs MPPT.

Different MPPT methods have been developed in the past. In this study, Perturb and Observe (P&O)-based MPPT is employed. The benefits of being straightforward, simple to use, and requiring little computation make this strategy the most popular one. This method continually modifies the array terminal's current and voltage while comparing the photovoltaic power output to the past power output as voltage is perturbed that direction if output power is enhanced; otherwise, it should be perturbed in the other way

4.6.2 VOLTAGE ORIENTED CONTROL (VOC) OF DC-AC VSI

A voltage-oriented control (VOC) strategy employing a proportional integral controller is described for utility - tied PV systems since the major goal of the grid-tied control system is to keep the output voltage sinusoidal and in phase with the output voltage that maintains close to unity power factor. This design, which is also referred to as direct power control, is based on the stationary reference theory and includes transforming three-phase ABC currents and voltages into a two-phase synchronous rotating frame (SRF) system that lags the grid voltage by 90 degrees. and, as a result, has a voltage of zero (Vq = 0). Park's transform is the name of the transformation type.

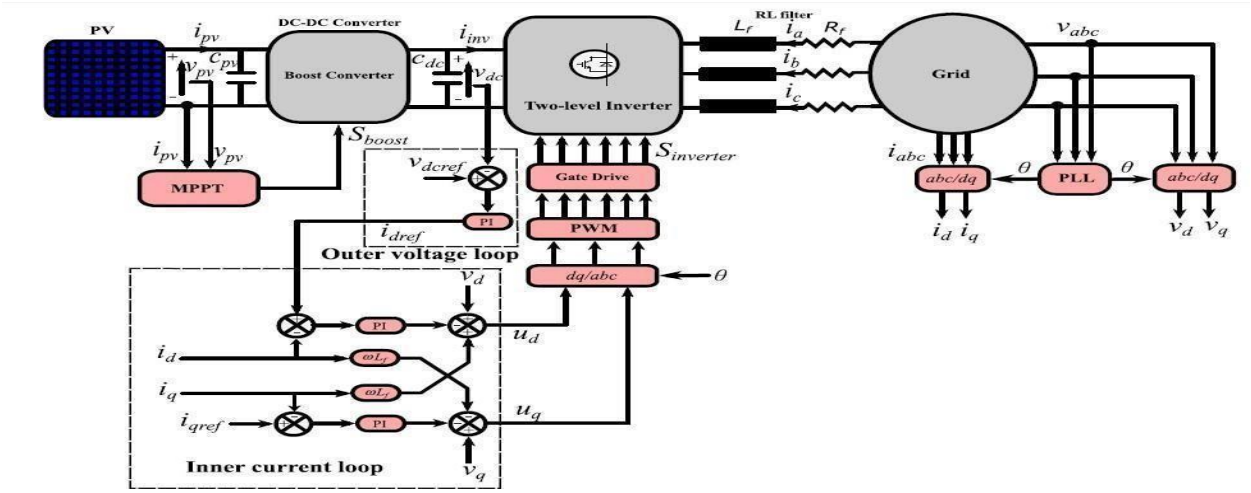

Fig. 4.5 Voltage oriented control approach

Two cascaded loops are used by the VOC to adjust the inverter control. A proportional controller is used to generate the reference current for the closed - loop system or current loop, and the DC-link capacitor voltage is connected to the outer loop or voltage loop

The reference current for the inner loop or current loop. The currents are then controlled by two PI controllers, enabling the active/reactive power control. Due of their strong transient reaction, predictive control approaches have recently attracted increased attention. In order to enforce specific tasks, additional criteria and constraints might be introduced to the algorithm. However, this control technique has some significant flaws, including a variable switching frequency and a heavy computational burden. Two loops are used in this control scheme: an inner current control loop and an outer voltage control loop. The reference value of q-axis current is taken to be zero in order to maintain a power factor that is close to unity. The following are the three-phase grid voltages and phase current formulae for a grid-tied inverter:

$$Va = Vm\cos\omega t \quad (4.1)$$

$$Vb = Vm\cos\omega t - 2\pi/3 \quad (4.2)$$

$$Vc = Vm\cos\omega t + 2\pi/3 \quad (4.3)$$

And

$$la = lm\cos\omega t \quad (4.4)$$

$$lb = lm\cos\omega t - 2\pi/3 \quad (4.5)$$

$$lc = lm\cos\omega t + 2\pi/3 \quad (4.6)$$

Figure 4.5 depicts the topology of a grid-tied inverter with an LC filter, where Va, Vb, and Vc represent voltages at the inverter end and Ua, Ub, and Uc represent voltages at the grid

$$Va = L\ dIa/\ dt + Ua \quad (4.7)$$

$$Vb = L\ dIb\ /dt + U \quad (4.8)$$

$$Vc = L\ dIc\ /dt + Uc \quad (4.9)$$

where L is the gird side filter's inductance value. and Ia , Ib, Ic are values of grid current. Utilizing Park's transformation, three-phase electrical current (Iabc) and voltages (Vabc) are converted to a two-phase synchronous rotating frame (SRF) dq0 system (Vdq0 and Idq0). These three-phase voltage values can be transformed into equation 10 of the dq transform as follows:

$$Vdq = Vd + jVq \quad (4.10)$$

$$Idq = Id + jIq \quad (4.11)$$

Apparent power can be presented as

$$S = 3/2\ (Vdq\ Idq\ *) \quad (4.12)$$

Where, Idq * is the complex conjugate of Idq.

Subsequently, the grid is supplied with the following active and reactive powers:

$$P = 3\ /2\ (Vd\ Id + Vq\ Iq) \quad (4.13)$$

$$Q = 3/\ 2\ (-Vd\ Iq + Vq\ Id\ ) \quad (4.14)$$

Since the grid is anticipated to be synchronized and the system to be in steady-state, Vq=0. Equation 4.14 is written as,

$P = 3/2\ (Vd\ Id\ )$ (4.15)

$Q = -3/2\ (Vd\mathrm{Iq})$ (4.16)

Here, reactive power's negative sign indicates that it might travel either from the grid to the inverter or the other way around. A PI controller is used in the outer voltage loop to control the dc-link voltage to a reference voltage that is a step signal, whilst an inner current control loop controls active and reactive current flow in a reference frame that is aligned with the grid's voltage vector. By measuring ABC grid voltages, a PLL is utilized to calculate the angle between grid current and voltage. Id and Iq values are compared to measured Id* and Iq* to manage the flow of active power. Figure 5 illustrates the usage of two PI controllers to give reference voltages for the q- and d-axes. (Vd, Vq) based on the q-axiscurrent Id and the d-axis current Iq.

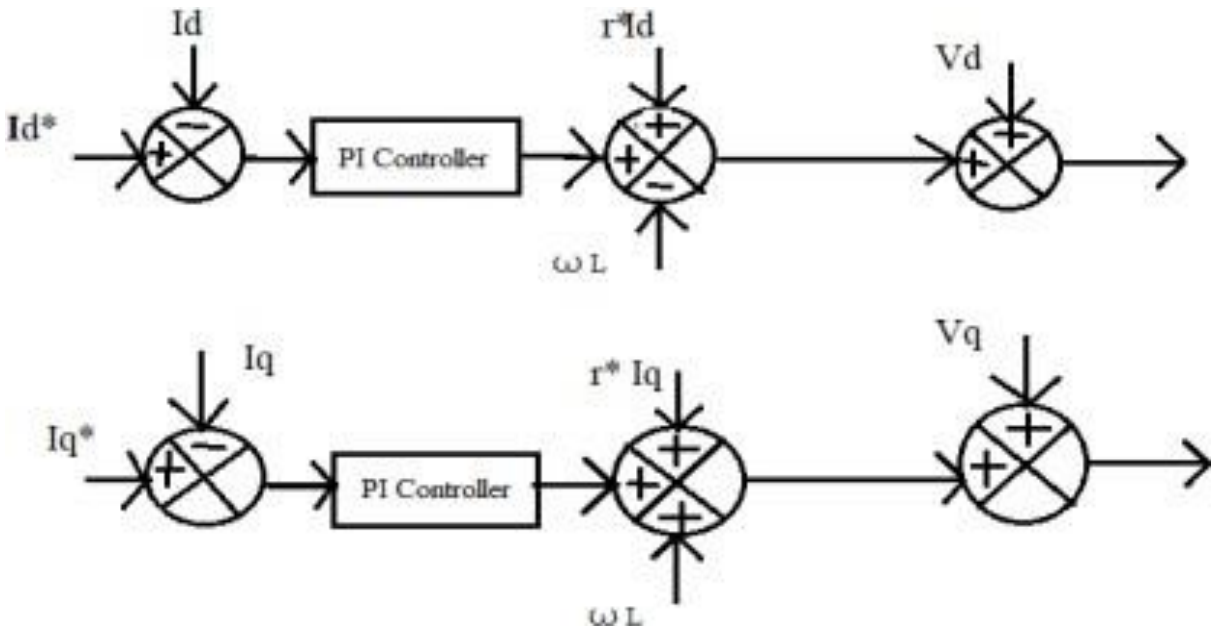

Fig. 4.6 PI controllers used to generate Vd*, Vq*

Lastly, an opposite dq axis to ABC base axis transformation is accomplished using Park's transform. Using an SPWM-based modulation approach using abc reference frame voltages, switching pulses are produced for the inverter. If either of the three-phase sinusoidal reference signals (Va, Vb, and Vc), which are 120* apart from one another, is greater than the triangle carrier signal Vc> Vt triangular, the inverter's switching pulse is either one or zero depending on the situation. predetermined value and offers the reference current for the current control loop. This is regarded as the traditional voltage-oriented voltage regulation approach.

CHAPTER 5

PROPOSED MODEL

5.1 INTRODUCTION

In this chapter, proposed system taken into consideration is studied. The sensorless control structure is formulated. To account for the loses occurring in the system, a loss model is created and implemented in the system. Dc link sensorless control strategies is utilized to control the two stage three phase inverters.

5.2 SENSORLESS POWER CONTROL

Modern control techniques increasingly use sensorless approaches because they improve system dependability. Additionally, in the event of a sensor failure, they can serve as a backup control

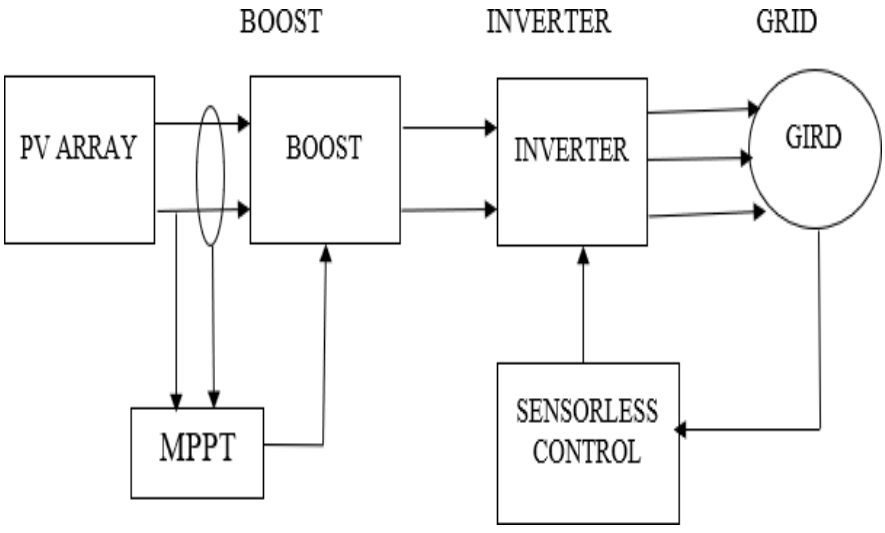

Fig.5.1 DC link sensorless control structure of microgrid connected P

Control methods without sensors have advantages. They actually provide the system with a host of capabilities. The system has a significantly lower cost when viewed from a

financial standpoint. Additionally, the control structure is simpler from a control perspective. In fact, to reduce the number of required sensors, some attempts have been done., leading to the development of sensorless control of the grid-connected inverter. The elimination of PV current and/or voltage sensors is the subject of some studies. However, this could result in a loss of maximum power extraction and degraded system behavior. DC-link sensorless control of PV systems have just recently been developed. A basic yet Model for actual losses in a two-stage grid-connected PV system is proposed in this project along with a sensorless DC-link control technique. In order to ensure a constant voltage at the inverter's input, the losses model takes into account the PV system's most significant losses. In order to account for unmodeled losses, Particle swarm optimization (PSO) was used to incorporate and enhance a further loss component. By eliminating the outside current loop, the reference current can therefore be calculated right away using the PV power generated and the developed losses model. The current generation is built on the hypothesis that feeding the extracted power from the PV source into the grid, which provides energy balance, will stabilize the DC-link voltage.

5.3 SYSTEM UNDER CONSIDERATION

The 3.8kW PV array of the grid-connected PV system is set up in series and parallel. A boost converter is used to raise the PV voltage to a useful level for grid integration after the PV source. Additionally, the MPPT is enacted using the fixed step one and the introducing flexible perturb and observe technique are contrasted. The sensorless DC-link voltage technology is used to control both the active and reactive current of the two-level inverter. The outside voltage loop is eliminated by this technique. The first stage consists of a VSI, which functions as a grid side converter, and a PV side boost converter. The solar PV array serves as the boost converter's input and is composed of modules connected in parallel and series to produce accurate voltage and current information and thus can be utilized.

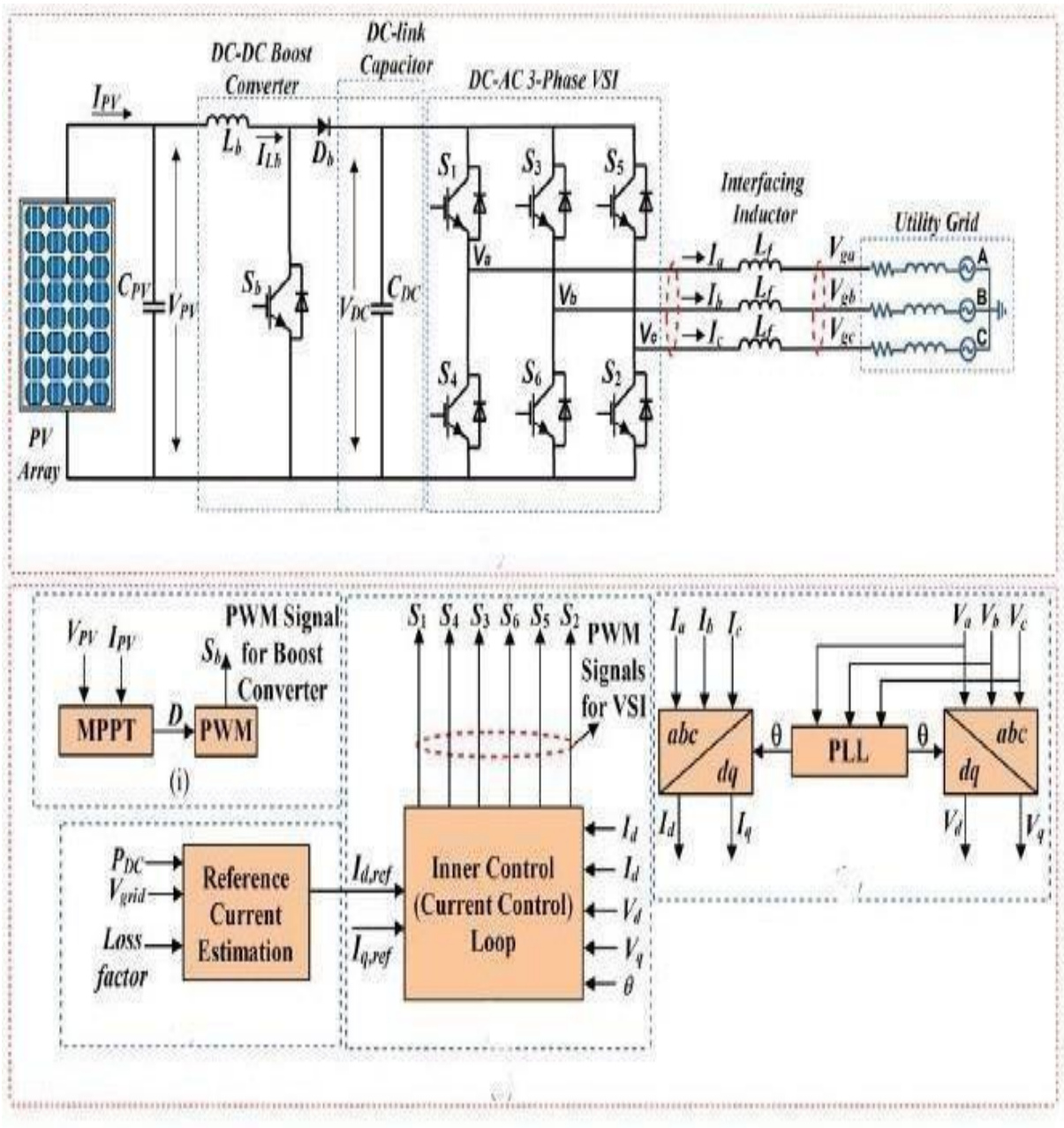

Fig..5.2 Control structure of grid connected PV system

As a converter in between a PV array and a VSI, the boost converter is used. It boosts the PV array's voltage level to ensure that VSI obtains an adequate voltage for the GCPVS. The operational points, VMPP (voltage at maximum power point) and IMPP (current at maximum power point) at corresponding PMPP, are chosen using the MPPT method (power at maximum power point).

5.4 MPPT CONTROL

The MPPT operating principle is crucial for PV systems. By using inverter control, the PV source's extracted power will be added to the grid. Under homogenous radiation circumstances, a definite maximum power point can be seen on the P-V curve, as seen in Fig. 5.3

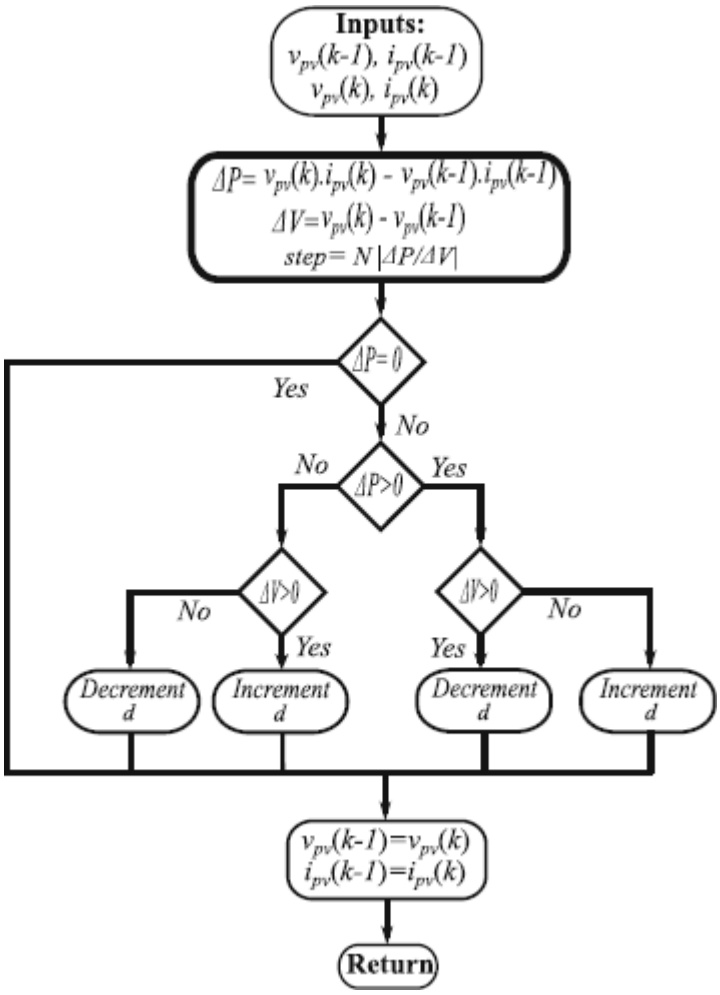

Fig. 5.3 Adaptive step size P&O algorithm

This point's location is constantly shifting as the atmosphere changes. So, the P&O method is used to track this location. The duty ratio (the control parameter) is perturbed by this procedure in one

way. For instance, the duty cycle is raised further if the power is increased. if not the duty cycle will be reduced in other case.

5.5 VOC BASED GRID CONNECTED INVERTER CONTROL

The grid voltage vector is aligned with the d axis to implement the VOC in the d-q reference frame.

The active and reactive currents (Equation (15)) in this instance can be stated as

$$P = (3/2)\, VdVq \tag{5.1}$$

$$Q = -(3/2)\, VqId \tag{5.2}$$

The active and reactive power are therefore separated from one another. As a result, by adjusting id and iq, respectively, Precise and standalone management of the active and reactive power is possible.

5.6 DC LINK SENSORLESS CONTROL TECHNIQUE

For the control of active and reactive power, the VOC has two cascaded loops. The proposed sensorless dc-link approach eliminates the outer loop by generating the reference current (idref) at the DC-link using the power balance technique. In order to ensure this equilibrium, a system's losses are examined using a created losses model. To ensure continuous DC-link voltage, It is necessary to achieve balance of power at the DC-link. The inverter DC link's power balance

$$Pd = Pinv + Pcapa \tag{5.3}$$

where Pinv is the immediate power supplied to the inverter, Pcapa is the immediate power from the Power converter, and Pd is the immediate power from the DC link input.

$$Pcapa = Vdc\ Cd\ cd/dt(Vdc) \quad (5.4)$$

where Vdc stands for the interval's DC-link voltage.

$$Pd = Pga\ (1- \cos(2wt)) + Vdc\ Cdcd/dt(Vdc) \quad (5.5)$$

Considering a unity power factor, Pga is the instantaneous active power provided into the grid. It is obvious that the DC-link capacitor comprises two power components. The first is the average power differenial between Pd and Pga, a DC component that affects the DC link voltage by linearly increasing or decreasing it. The DC-link voltage experiences a double line-frequency ripple as a result of the grid power ripple, which is twice as fast as the AC mains frequency. The DC-bus capacitor should smooth out these power variations and reduce voltage ripple. Without using an external DC-link voltage control loop, the DC- link voltage is stabilized and can be changed. The control mechanism presented here senses the PV current and voltage to produce MPPT. How much the standard grid current is increased depends on the logged maximum PV power value. The maximum PV power that was tracked and is represented by a sinusoidal current that is produced by the inverter under the influence of the grid current controller and has a magnitude that is equal to that of the reference current. In order to meet the power balance at the inverter DC-link, the maximum PV power is therefore compelled to flow to the inverter AC side, causing a voltage regulator to not be required, allowing the DC-link voltage to spontaneously to become steady at a certain level.

5.7 1 EXLUDING SYSTEM LOSS COMPENSATION

In order to establish power balance at the ac-dc converter DC link and have without the requirement for a DC-link voltage regulator, Vd is intrinsically stable, the suggested control techn-

que must ensure that the tracked PV system's maximum power is transferred to the grid. Consequently, is calculated by multiplying the maximum photovoltaic power at a specific Grid current rms value divided by ecological conditions (PPV) (Vg). Following this, a sinusoidal pattern is used to multiply this intensity by the grid voltage produced via PLL. The grid current Compensator, which is similar to the one used in the traditional control technique, forces the inverter to generate a continuous power flow that fits this reference the control loop for uncompensated grid current.

$$Ig = \sqrt{2}\, P_{pv}/Vg \qquad (5.6)$$

This uncompensated approach, however, ignores system losses, such as those caused by the parasitic serial resistance in Cdca and the converter power electronics switches. As a result, there is an imbalance in the balance of power at the DC-link and the DC-link current drops below the grid voltage amplitude. This causes the modulation index (ma) to increase and possibly reach unity, which will cause as will be demonstrated at the end of this paragraph, oscillations in the grid current can exceed permitted limits.

5.7.2 WITH LOSSCOMPENSATION IN SYSTEM

In reality, the system loses some of this power (Ppv). As a result, when all the electricity is put into the grid, the DC-link voltage decreases. The pulse width modulated signals' modulation index may cross unity as a result of such decrease. As a result, the currents' total harmonic distortion (THD) will exceed acceptable levels and the inverter's output voltage will be warped.

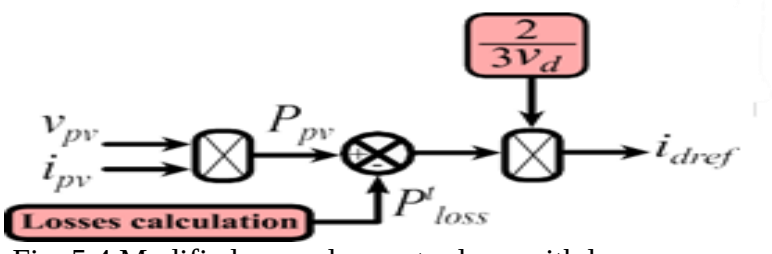

Fig. 5.4 Modified sensorless outer loop with loss compensation

Additionally, the power that is injected will be of lower quality. Therefore, it is essential to factor in the losses of the PV system. These losses can be assessed as well as categorized into converter losses and inverter losses.

$P^{1}loss = Pconv + Pinv$ (5.7)

This can be further evaluated as per the generated losses model.

$P^{1}loss = i\ 2l\ Rl + ilvs + 2vsidc$ (5.8)

where idc represents the average value of iinv and il equals ipv.

Here considered system is simulated twice— To find the ideal Dc input voltage, several DC-link voltage levels and irradiance levels were checked extensively using the recommended DC-link voltage observer - based technique and again using the conventional control technique. The first scenario's steady-state performance (in terms of THD and power generation losses) is supplied using the conventional method. The converter loss and grid current THD levels are both directly impacted by the DC-link voltage value. THD exceeds acceptable levels when Vdc=600V, or ma>1, whereas it does not for Vdc=620V.

The grid current control, which is the primary controllable variable for the VSI, is accomplished using a Proportional-Resonant (PR) controller in both the traditional and the proposed control systems. Due to the nature of PR regulators, which work with harmonic waves, the grid voltage amplitude and frequency must match in order for the grid current to converge to its reference. The grid current control PR controller emits a sinusoidal signal. As a result, the grid current output controller output serves as the modifying signal Vmsina for the development of VSI SPWM. The constant pitch carrier signal Vmtri VSI modulation index ma causes linear fluctuations in the grid current PR regulator output signal Vmsina. After the proportional resonant controller block, a straightforward limiter is added to prevent over- modulation by capping the modulation index at 1. Additionally, at the same amount of irradiance, device loss increases as Vdca grows (i.e., fixed

PPV). The latter limits how much energy may be transmitted overall to the grid. The steady-state results for the uncompensated and compensated systems for two DC-link voltage levels at various irradiance levels are presented for the second example utilizing the suggested observer - based technique. These findings deal with grid power losses and grid side total harmonic distortion.

CHAPTER 6

SIMULATION

6.1 INTRODUCTION

With the use of a MATLAB-Simulink model, the entire microgrid connected PV system is simulated in order to assess the viability of the VOC scheme and dc link sensorless power control scheme. A solar panel of the solartech1Std445P type is utilized for modelling purposes, with 3 modules connected in series and 6 parallel strings. The irradiance values are 1000 W/m^2. Figure depicts the entire three phase MATLAB/Simulink model.

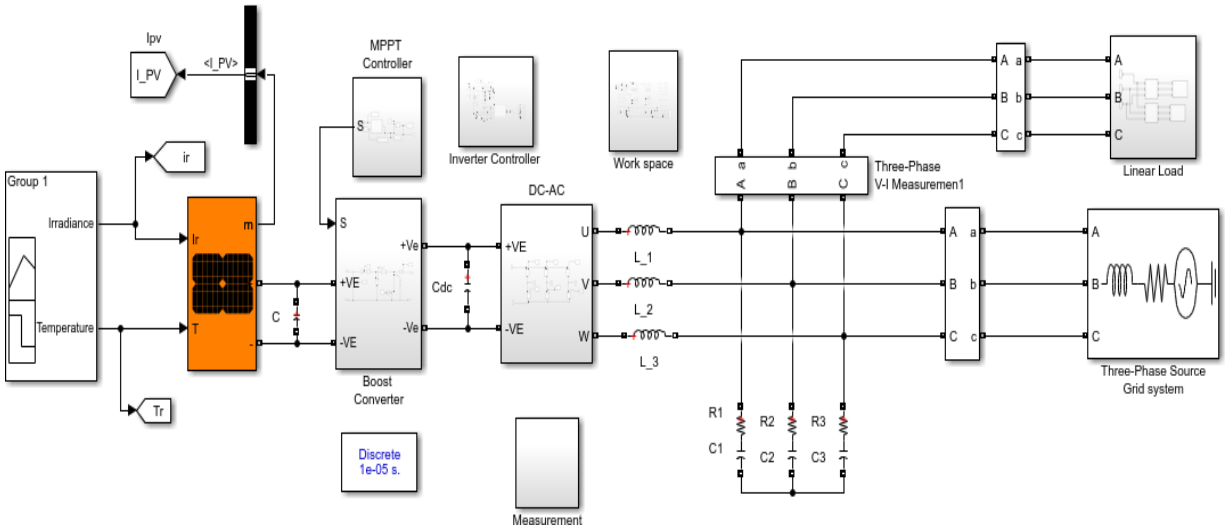

Fig. 6.1 Simulation diagram of microgrid connected PV systems

The PV voltage is increased to 600V with the aid of a boost converter for grid integration after the PV voltage is increased to 600V with the aid of a boost converter for grid integration after the PV source. Moreover, maximum power point tracking is implemented using an adaptive step-size

perturb and observe technique. The output of boost is fed to a two-stage inverter, which then is connected to microgrid maintained at 400V.

Table 6.1 System parameters taken for the design

PARAMETERS	VALUE
PV array power(kW)	3.8
Boost inductance	3.73mH
Switches and diode drops	1V
Switching frequency(kHz)	10
DC link capacitance	10μF
Filter Inductance	25mH
Filter resistance	0.1Ω
Grid current frequency	2Π*50 rad/s
Grid line voltage	400V
Sampling time	40μS
Boost capacitance	13.190 μF

6.2 PV SYSTEM DESIGN

Open circuit voltage, Voc=49.89V Short circuit current, Isc =11.41A

PV voltage, Vpv = open circuit voltage × number of panels in series

$$= 49.89 \times 4 \quad (6.1)$$

PV power, Ppv = 445× number of panels (9)

$$= 3.8Kw \quad (6.2)$$

6.3 DESIGN OF BOOST CONVERTER

Input voltage, Vin = Vpv = 199.89V

Output current, Iout = Pout/ Vout = 3.8k/ 600 = 5.933A (6.3)

Input current, Iin = P/ Vin =3.8k/199.56 = 17.871A (6.4)

Duty ratio, D = (Vo -Vin) / Vo = (600-199.56)/600 = .667 (6.5)

Assume 20% of current ripple

$\Delta I_L = 0.2 \times I_{out} \times (V_{out}/V_{in})$

$= 0.2 \times 5.933 \times (600/199.56)$

$= 3.57A$ (6.6)

$$\text{Inductance, } L = \frac{V_{in}(V_{out}-V_{in})}{I_L \times f_s \times V_{out}}$$

$$= \frac{199.56(600-199.56)}{3.66 \times 10K \times 600}$$

$= 3.73mH$ (6.7)

$$\text{Capacitance, } C = \frac{I_o \times D}{F_s \times \Delta V_{out}}$$

$$= \frac{6.083 \times 0.668}{10k \times 0.05 \times 600}$$

$= 13.1910\mu F$ (6.8)

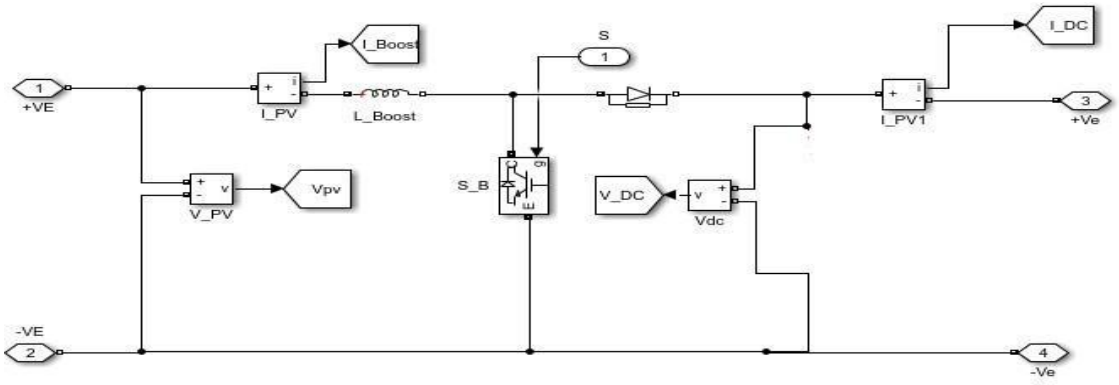

Fig. 6.2 Simulation of boost converter

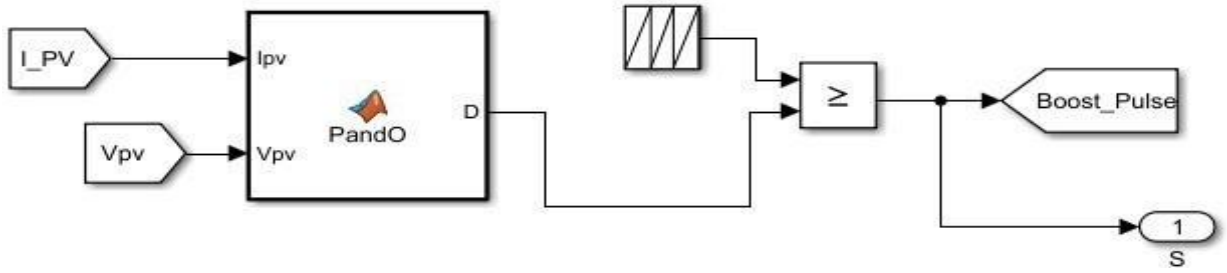

Fig. 6.3 Simulation of boost pulse with MPPT

Adaptative perb and observe algorithm is used for MPPT implementation. Here MPPT is implemented in this boost converter by sensing both pv current 11.41A and voltage 200 by the respective sensors and by using these values, mppt is implemented. The output of the mppt will directly give the duty ratio which is .66 for the pulse width generation. This duty ratio value is compared with carrier signal and is given to the gate terminal of MOSFET.

6.4 DESIGN OF FILTER ON GRID SIDE

$$\text{Capacitance, } C = \frac{Q \times (P/3)}{V_{out} \times \omega} = \frac{0.05 \times (3.5k/3)}{415 \times 2\Pi \times 50}$$

$$= 44.765\ \mu f \qquad (6.9)$$

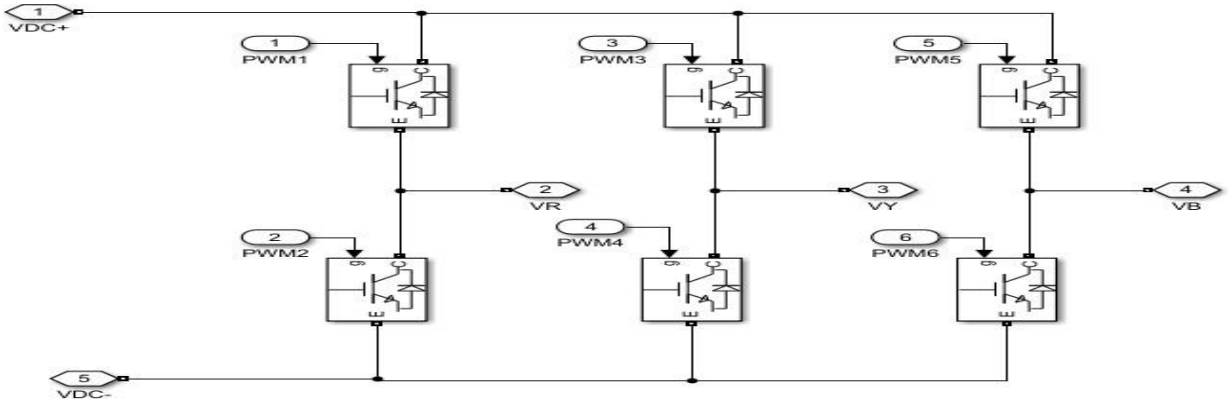

Fig. 6.4 Six pulse inverter topology

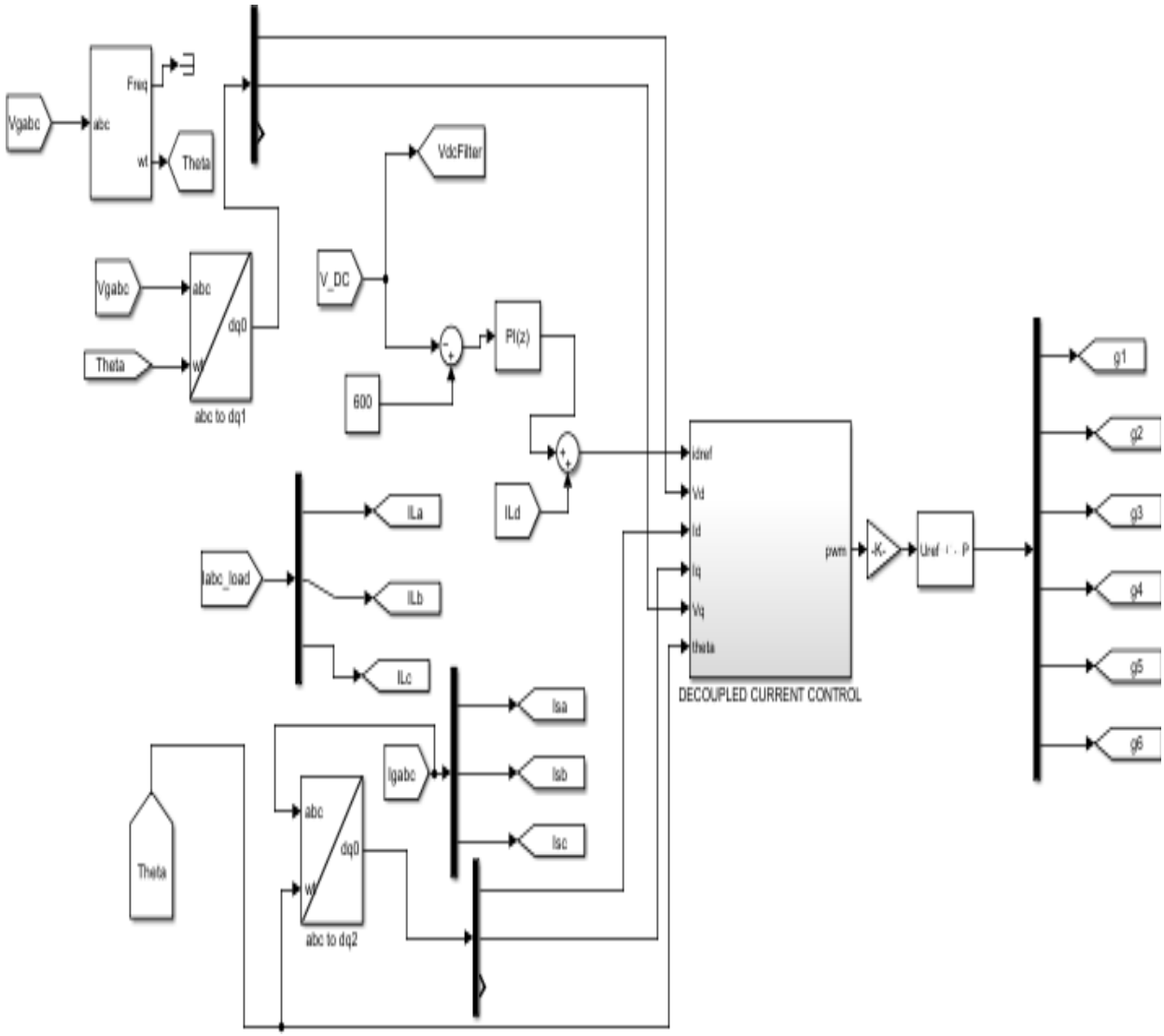

Fig. 6.5 Simulation diagram of voltage-oriented control (VOC)

In the outer loop, DC link voltage is measured by using a voltage senor and is compared with reference voltage 600V and is given to a proportional integral controller to reduce steady state error and peak overshoot. The reference current generated by the PI controller which then is fed to the inner loop of the inverter control structure. The inverter topology here used is 6 pulses so need six pulse generation for the gates of two stage inverter.

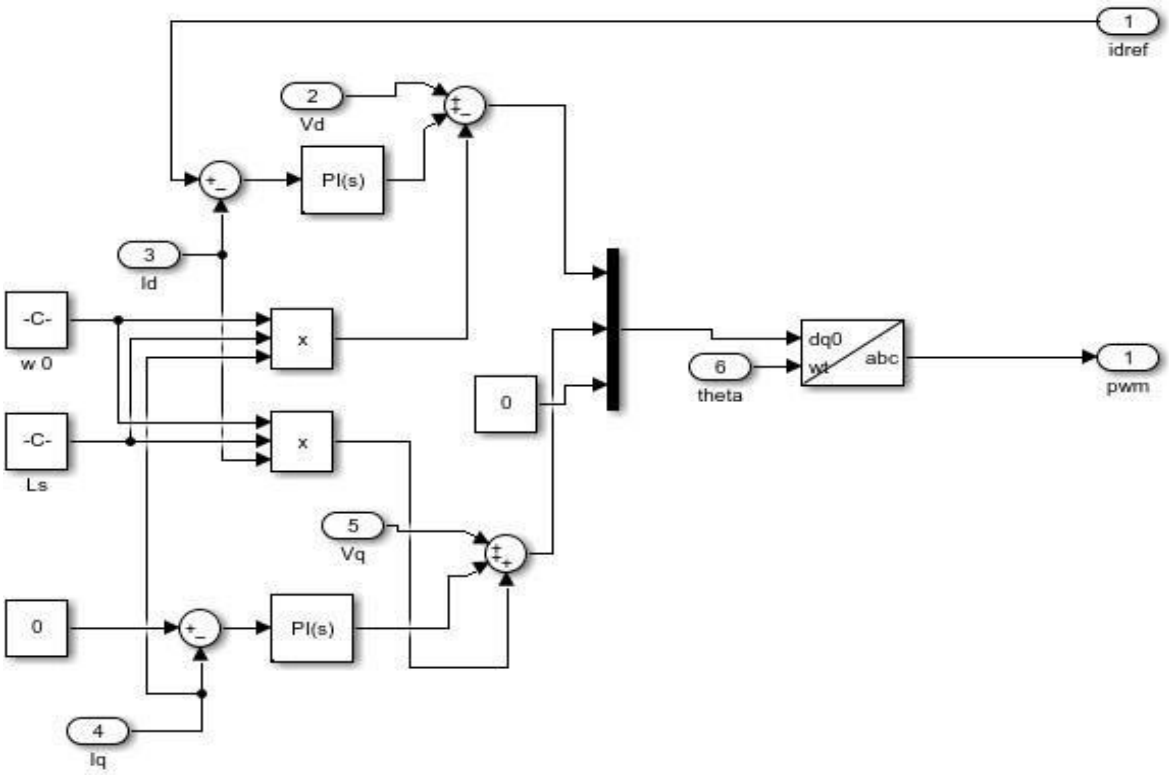

Fig. 6.6 Simulation of inner current control loop

The reference current idref generated in the voltage loop is now fed to the inner loop where this reference current is compared with the active current Id and the error is fed to a proportional integral controller to generate Ud. Similarly, the reactive current and the reference reactive current is compared and fed to PI controller to generated Uq. This Ud and Uq are scaled and given to a pulse width generator along with angle information to generate the six pulses for the inverter.

6.5 SIMULATION OF SENORLESS CURRENT CONTROL

In sensorless control, instead of comparing reference voltage (600V) and dc link voltage (designed for 600V, measured by voltage sensor) to generate reference current, here a loss model is created which then compare with maximum pv power(3.8kW) and inverter power along with $2/3^{rd}$ of maximum grid voltage. The output of this modified outer loop is fed to the current loop to control the active and reactive current.

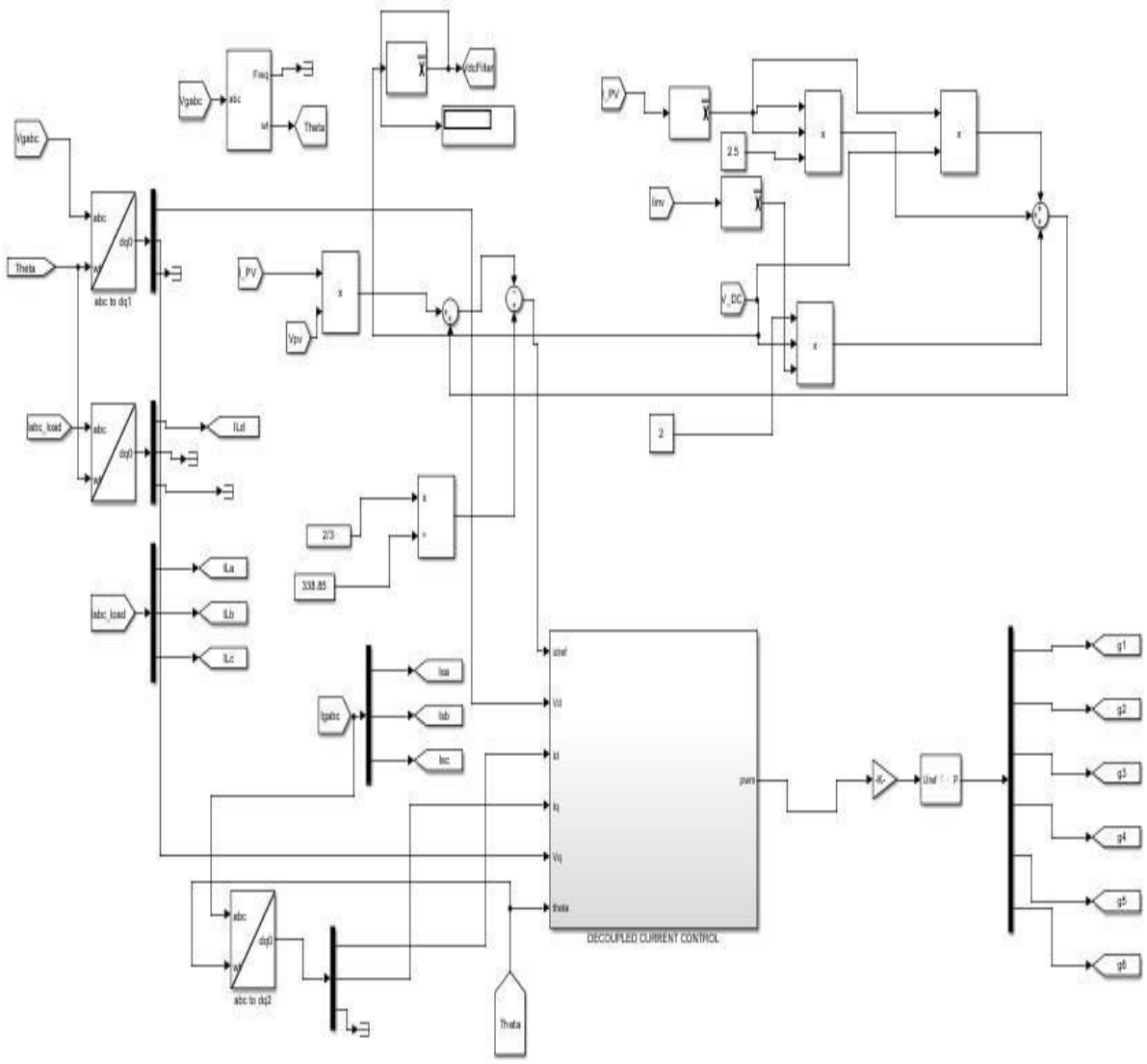

Fig. 6.7 Simulation diagram of Sensorless current control in inverter

CHAPTER 7

RESULTS AND DISCUSSION

7. 1 INTRODUCTION

This chapter discusses the transient response, speed of the response, the stability of the system with conventional voltage-oriented control and sensorless power control design.

7.2 ANALYSIS OF PV ARRAY

The waveforms display the PV Power generation, its voltage, and current at a constant temperature of 25 °C under various irradiance. Adaptive perb and observe reduces oscillations in steady state, improving the algorithm's efficiency. The PV voltage waveform under normal P& O has higher over shoots and cause high ripple in the PV power.

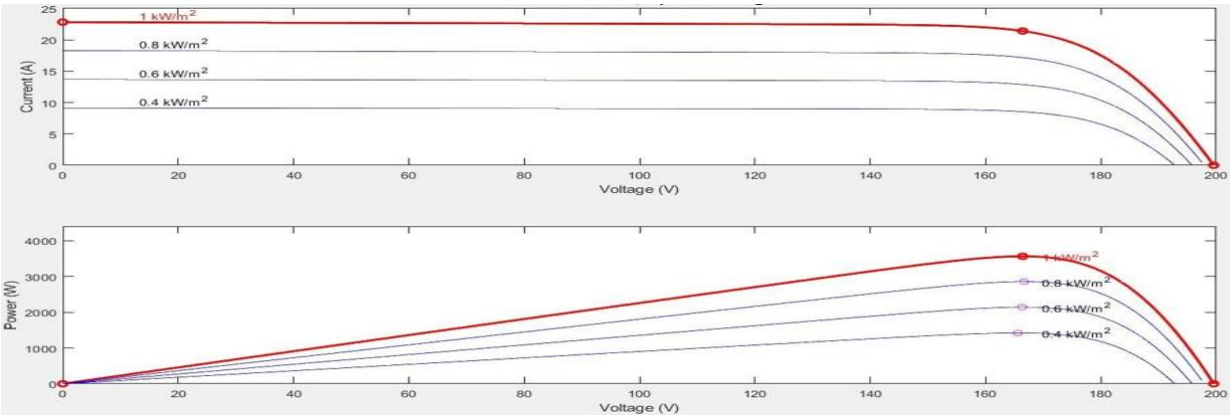

Fig. 7.1 The pv module's I-V and PV statistics at various irradiances

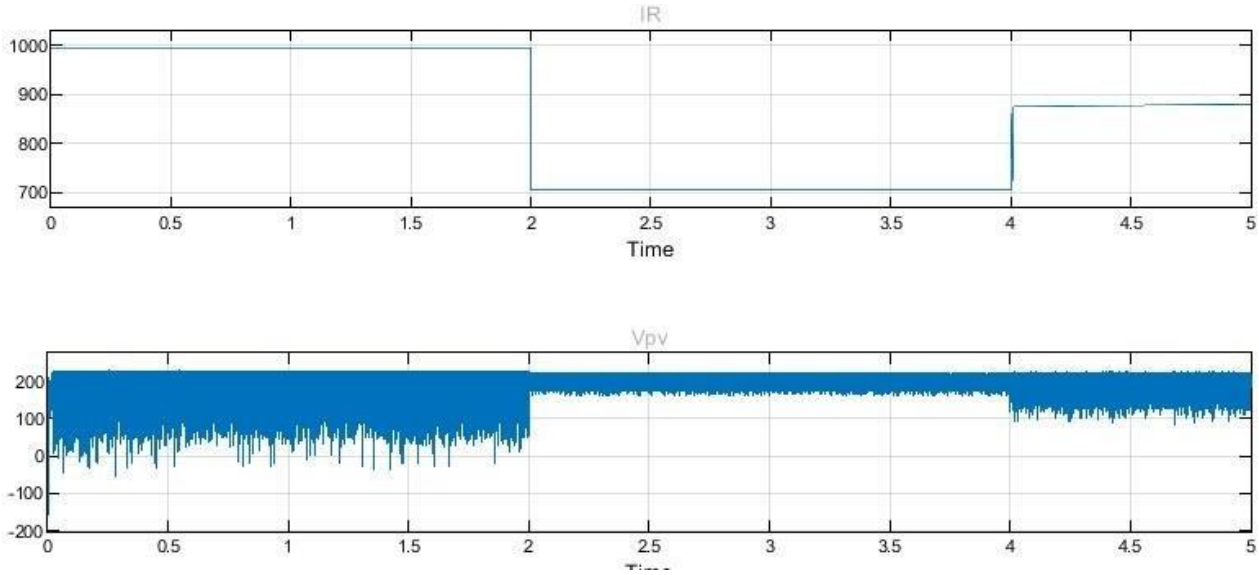

Fig. 7.2 Irradiance and PV voltage at 1000 w/m^2 and 700 w/m^2

At 1000w/m2 irradiance maximum pv voltage of 200V is obtained. As the irradiance level drops so do the power drops and thus the losses occurring in the system reduces and thus the compensation current is less. In conventional system the undershoot occurring for pv voltage is as low as 167V.

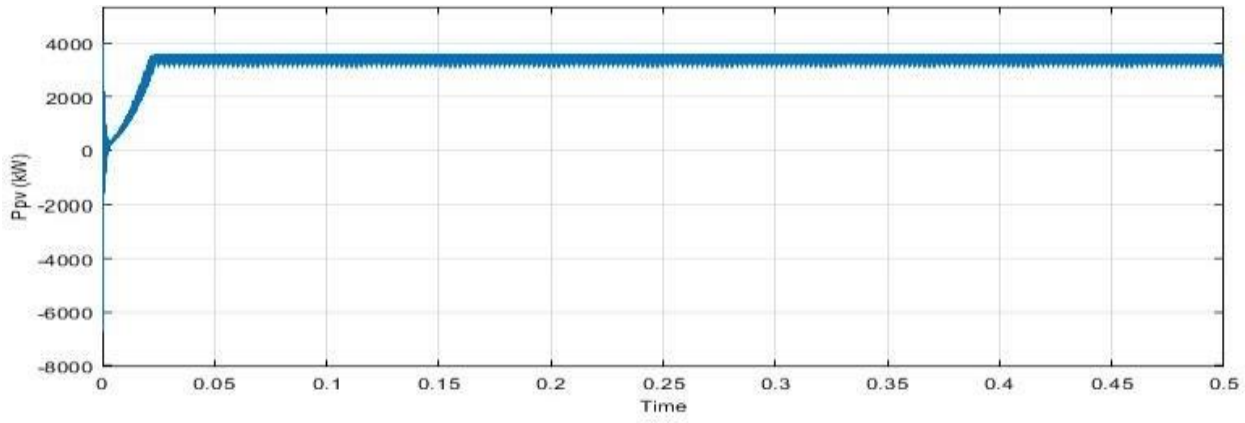

Fig. 7.3 PV power of the microgrid connected PV system

For 1000w/m2 irradiance the pv power output obtained is 3.8kW. The peak undershoot in conventional stem is as low as 3101kW.

7.3 COMPARISON OF COVENTIONAL AND PROPOSED CONTROL SCHEME

Dc capacitor voltage, pv power, response of the system during load switching are compared to evaluate the performance of the proposed system.

7.3.1 DC LINK VOLTAGE RESPONSE

The sensorless response of the dc link voltage is compared to the Vdc response in the conventional technique. In the voltage-oriented method, Vdc is compared with reference 600V to generate the reference current. The dc link voltage settles at value 593V which is less than 600V because of the losses occurring in the system but gets stabilized at this magnitude as inner active and reactive currents are in synchronous with Grid.

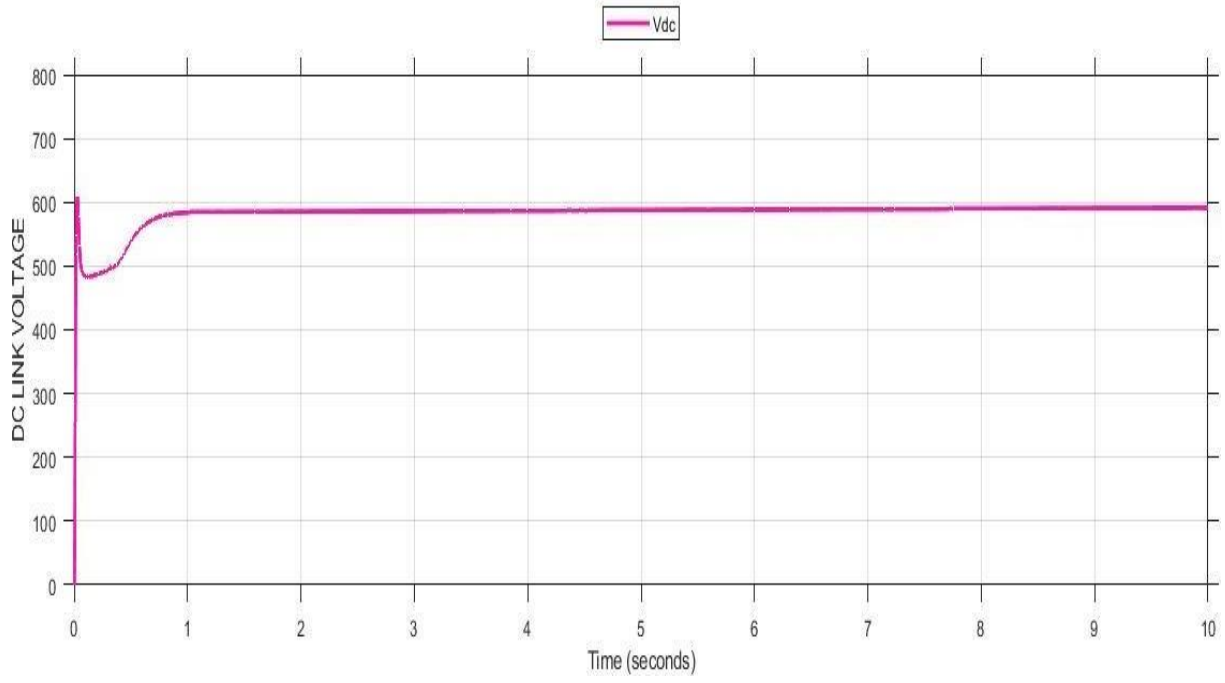

Fig. 7.4 DC link voltage with a voltage-oriented control.

In proposed system the voltage settles at 600V. This is based on the fact that power balance technique is implemented in the system such that any power loss occurring in the system is compensated. The undershoot occurs here because in order to reduce the complexity of the system the controller is removed.

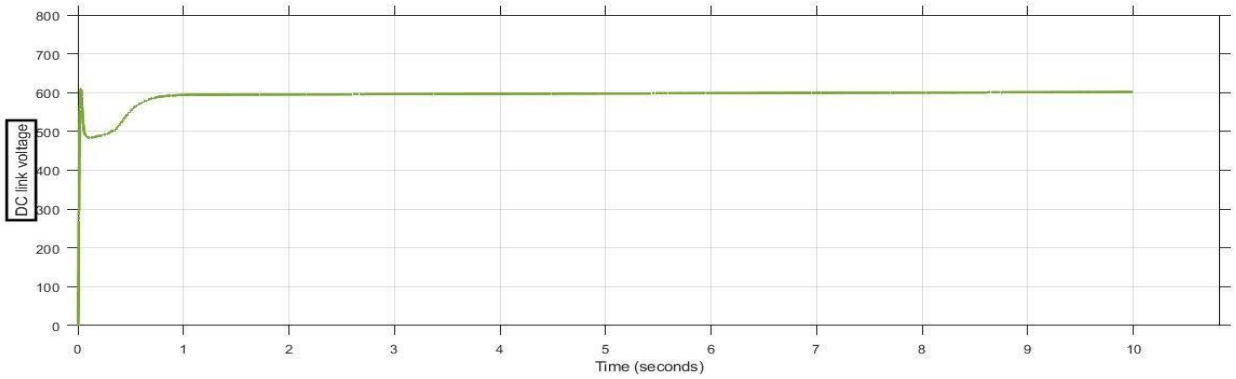

Fig. 7.5 DC link voltage with a proposed power control.

7.1.1 PHOTOVOLTAIC POWER RESPONSE

Despite the two approaches using the same PI controller values for the current loop, the PV power of the conventional VOC displays a higher over shot than the one proposed. Additionally, under irradiation condition, the typical VOC exhibits a slightly slower transient reaction in comparison to the proposed sensorless approach so that the PV power experiences a slower transient and a somewhat larger ripple content.

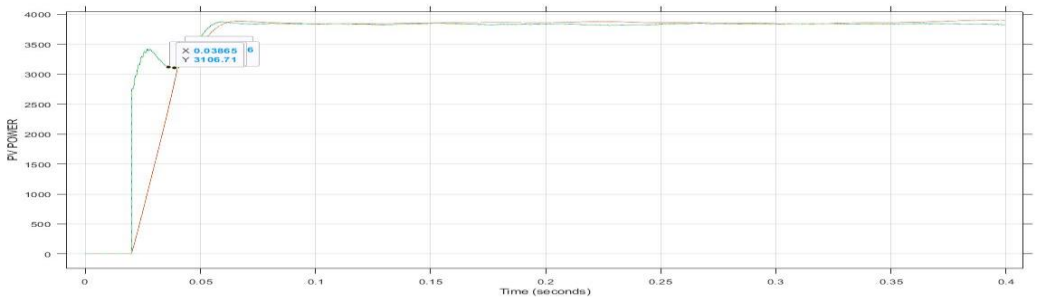

Fig. 7.6 Transient response comparison of VOC

A slower transient nature is found in conventional voltage-oriented system at the event of load addition. Here a load of 4.2kW is added at 2 sec. It takes 0.118 sec to respond to load addition to supply required active power. Another load of 2.7kW is added after 0.5 sec and it takes 0.681sec to respond to the load addition. Similarly, both the load is switched off at 5 sec and takes nearly 0.24 sec to respond to reduce the power to zero.

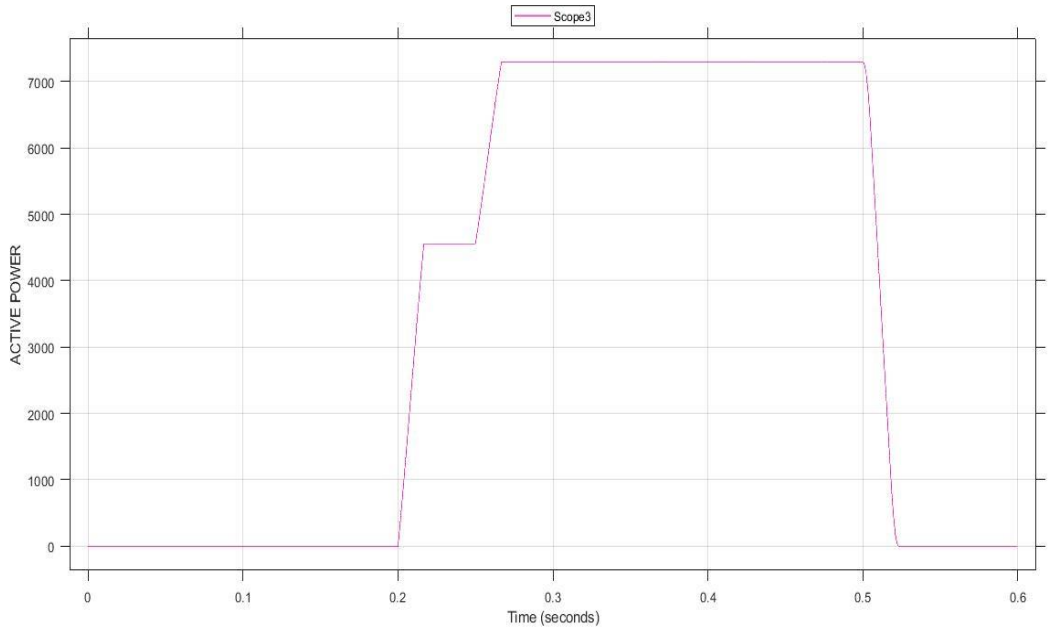

7.7. Time response of VOC during load addition.

Comparing the proposed system to the sensorless system, the sensorless system responds to the system quickly as the load of 4.5kW and 2.7kW is added to the system at 2.5s and 3s, respectively i.e., it takes 0.0168s to respond when load is switched off at 5sec system takes 0.01 sec to respond. This shows that the proposed system responds after to load switching.

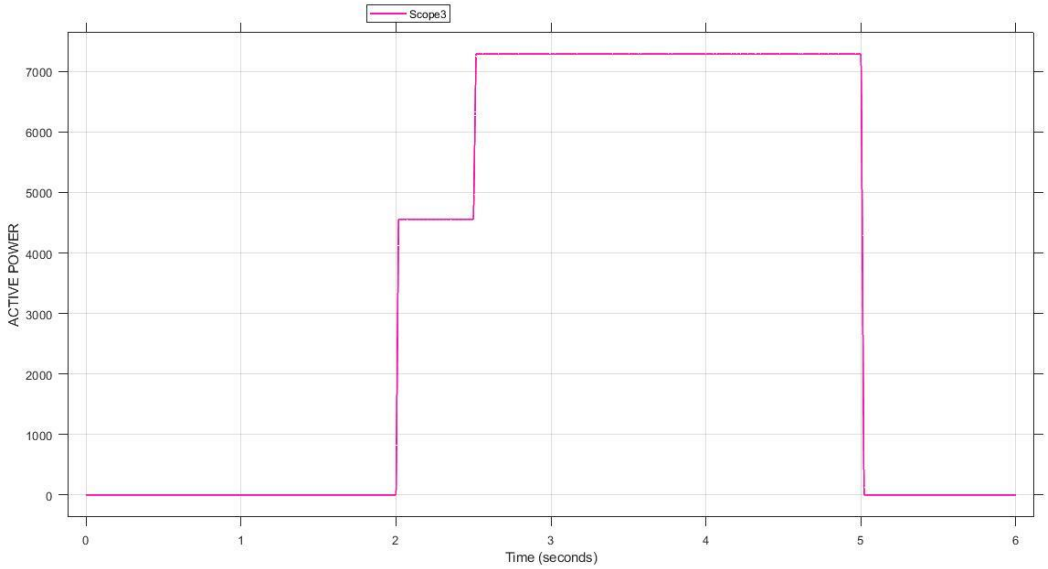

Fig. 7.8 Time response of proposed system during load addition

CHAPTER 8

CONCLUSION

In this work, a unique sensorless DC-link voltage technique for three-phase two-stage, GCPVS is developed. By avoiding the outer control loop, this technique produces an operational reference current for the production of PV power using a novel DC-link voltage control model. Therefore, the estimated value is used to achieve power balance and DC-link voltage remains constant. Instead of employing a fixed step, to reduce any possible steady flow oscillations, the MPPT is regulated using an adaptive step-size P&O method. By removing the outer PI controller loop, In this study, the conventional tumbled VOC loops are not used, resulting in the sensorless DC-link control technique. By building a detailed model of the system's losses, the proposed method assures the balance of power at the DC-link. The power that should be injected into the grid is then calculated by deducting the losses from the system's MPPT scheme. With no requirement for the outside PI controller, the reference current can thus be directly approximated. The DC-link voltage sensor is eliminated by the suggested method. As a result, the system's cost is lower and its dependability is increased. Additionally, the overall control structure is simplified by eliminating the cross - coupled loops of the conventional VOC. The findings demonstrate that, in comparison to the conventional approach, the proposed sensorless solution has a better transient response under most operating situations. Additionally, the PV power overshoots are significantly decreased. Finally, the proposed technique improves the quality of the injected power and offers a better response to load change.

REFERENCES

1. **Mostafa Ahmed, Mohamed Abdelrahem, Ahmed Farhan, Ibrahim Harbi, Ralph Kennel** 'DC-link sensorless control strategy for grid-connected PV systems' electrical engineering ,2021,10(103:2345–2355)
2. **Abd Rahim N, Selvaraj J**(2007) Hysteresis current control and sen- sorless MPPT for grid-connected photovoltaic systems. In: 2007 IEEE international symposium on industrial electronics, pp 572-577. IEEE
3. **Ayan Mallik, Alireza Khaligh** DC Link Voltage Sensorless Control of a Three- Phase Boost Power Factor Correction Rectifier. Transactions on Power Delivery Vol. 35, no. 4, pp. 2011-2020, Aug. 2016
4. **Nor Azizah Yusoff, Azziddin M. Razali, Kasrul** A Concept of Virtual-Flux Direct Power Control of Three-Phase AC-DC Converter International Journal of Power Electronics and Drive System (IJPEDS) Vol. 8, No. 4 pp. 1776~1784, December 2017.
5. **N.E. Zakzouk, A.K. Abdelsalam, A.A. HelalPV** Single Phase Grid Connected Converter: DC-link Voltage Sensorless Prospective. IEEE Journal of Emerging and Selected Topics in Power Electronics (Volume: 5, Issue: 1, March 2017)
6. **Rodriguez J, Silva C** Dc voltage sensorless control method for three-phase grid-connected inverters. IET Power Electron., Vol. 3, Iss. 4, pp. 552–558, May 2010.
7. **Zanchetta P, Cortes P, Perez M,** (2011) Finite states model predictive control for shunt active filters. In: IECON 2011-37th annual conference of the IEEE industrial electronics society, pp 581-586. IEEE
8. **Alajmi Panwar NL, Kaushik SC, Surendra K** (2011) Role of renewable energy sources in environmental protection: a review. Renew Sus- tain Energy Rev 15(3):1513–1524
9. **Marco L, Thilo S, Hung John Y** (2010) Future energy systems: integrating renewable energy sources into the smart power grid through industrial electronics. IEEE Ind Electron Mag 4(1):18–37

10. **Atika Q, Fayaz H, Rahim Nasrudin ABD, Glenn H, Daniyal A, Khaled S, Khalid H** (2019) Towards sustainable energy: a system- atic review of renewable energy sources, technologies, and public opinions. IEEE Access 7:63837–63851
11. **Sahu Bikash Kumar** (2015) A study on global solar PV energy developments and policies with special focus on the top ten solar PV power producing countries. Renew Sustain Energy Rev 43:621– 634
12. **Aguilera Ricardo P, Quevedo Daniel E, Vzquez Sergio, Franquelo Leopoldo G** (2013) Generalized predictive direct power control for ac/dc converters. In: 2013 IEEE ECCE Asia Downunder, pp 1215-1220. IEEE
13. **Yongchang Z, Zhengxi L, Yingchao Z, Wei X, Zhengguo P, Chang- bin H** (2012) Performance improvement of direct power control of PWM rectifier with simple calculation. IEEE Trans Power Electron 28(7):3428–3437
14. **Atika Q, Fayaz H, Rahim Nasrudin ABD, Glenn H, Daniyal A, Khaled S, Khalid H** (2019) Towards sustainable energy: a system- atic review of renewable energy sources, technologies, and public opinions. IEEE Access 7:63837–63851